

**METHODS AND INSTRUMENTATION
FOR QUANTITATIVE MICROCHIP
CAPILLARY ELECTROPHORESIS**

Tobias Revermann

Members of the committee:

| | | |
|---------------------|----------------------------|---------------|
| Chairman/Secretary: | prof. dr. ir. J. Huskens | Univ. Twente |
| Promotor: | prof. dr. U. Karst | Univ. Twente |
| Members: | prof. dr. H. Gardeniers | Univ. Twente |
| | prof. dr. H.-U. Humpf | Univ. Münster |
| | dr. ir. W. Olthuis | Univ. Twente |
| | prof. dr. B. J. Ravoo | Univ. Münster |
| | prof. dr. B. Wenclawiak | Univ. Siegen |
| | prof. dr. ing. M. Wessling | Univ. Twente |

Print: PrintPartners Ipskamp, P.O. Box 333, 7500 AH Enschede,
The Netherlands

© Tobias Revermann, Enschede, 2007

No part of this work may be reproduced by print, photocopy or other means
without permission in writing of the author.

ISBN: 90-365-2457-1

**METHODS AND INSTRUMENTATION
FOR QUANTITATIVE MICROCHIP
CAPILLARY ELECTROPHORESIS**

DISSERTATION

to obtain

the degree of doctor at the University of Twente,

on the authority of the rector magnificus,

prof. dr. W.H.M. Zijm,

on account of the decision of the graduation committee,

to be publicly defended

on Friday February 2nd, 2007 at 13.15

by

Tobias Revermann

born on April 27th, 1977

in Osnabrück, Germany

The dissertation has been approved by the promotor:

prof. dr. Uwe Karst

Contents

| | |
|--|----------|
| Abbreviations | v |
| Chapter 1 Introduction | 1 |
| 1.1 Introduction and scope | 1 |
| 1.2 References | 4 |
| Chapter 2 Microchip Capillary Electrophoresis for Quantitative Analysis | 5 |
| 2.1 Introduction | 6 |
| 2.2 General aspects for the quantification on microchips | |
| – differences of CE and MCE | 9 |
| 2.3 Electrolysis and electrode effects | 14 |
| 2.4 Bubble formation and particles | 20 |
| 2.5 Surface interactions and materials | 22 |
| 2.6 Injection and Power supply | 25 |
| 2.7 Detector related problems | 26 |
| 2.8 Problem solving in MCE | 28 |
| 2.9 Future challenges and opportunities | 30 |
| 2.10 References | 31 |

| | |
|---|-----------|
| Chapter 3 Extendable four channel high-voltage power supply for fast microchip capillary electrophoretic separations | 37 |
| 3.2 Experimental | 41 |
| 3.2.1 Electronic components | 41 |
| 3.2.2 Chemicals, microchips and detection system | 42 |
| 3.3 Results and Discussion | 44 |
| 3.3.1 Construction of the HVPS | 44 |
| 3.3.2 Operation of the HVPS | 49 |
| 3.3.3 Electrophoretic separations | 49 |
| 3.4 Conclusions | 52 |
| 3.5 References | 56 |

| | |
|--|-----------|
| Chapter 4 Quantitative Analysis of Thiols in Consumer Products on a Microfluidic Capillary Electrophoresis Chip with Fluorescence Detection | 57 |
| 4.1 Introduction | 58 |
| 4.2 Materials and methods | 62 |
| 4.2.1 Materials, chemicals and samples | 62 |
| 4.2.2 Buffer and standard preparation | 63 |
| 4.2.3 Derivatization procedure and sample preparation | 63 |
| 4.2.4 CE, MCE and HPLC separation conditions | 64 |
| 4.2.5 Fluorescence microscope and data analysis | 67 |
| 4.3 Results | 68 |
| 4.3.1 Fluorescence properties of SBD-thiol derivatives | 68 |
| 4.3.2 Optimization of electrophoretic separations | 71 |
| 4.3.3 Microchip separations | 73 |
| 4.3.4 Comparison of HPLC, CE and MCE measurements | 77 |
| 4.3.5 Quantification of thiols in depilatory cream and cold wave lotions | 78 |
| 4.4 Conclusions | 81 |
| 4.5 References | 82 |

| | |
|---|------------|
| Chapter 5 Quantitative On-Chip Determination of Taurine in Energy and Sports Drinks | 85 |
| 5.1 Introduction | 86 |
| 5.2 Experimental | 89 |
| 5.3 Results and discussion | 93 |
| 5.4 Conclusion | 101 |
| 5.5 References | 102 |
| | |
| Chapter 6 Bilayer Vesicles of Amphiphilic Cyclodextrins: Host Membranes that Recognize Guest Molecules | 105 |
| 6.1 Introduction | 107 |
| 6.2 Materials and Methods | 111 |
| 6.3 Results and Discussion | 113 |
| 6.4 Conclusions | 120 |
| 6.5 References | 121 |
| | |
| Chapter 7 Concluding remarks and future perspectives | 125 |
| | |
| Summary | 127 |
| | |
| Samenvatting | 129 |

Abbreviations

| | |
|--------|--|
| ACN | acetonitrile |
| CCD | charge-coupled device |
| CE | capillary electrophoresis |
| CZE | capillary zone electrophoresis |
| DAD | diode-array detector |
| DMSO | dimethyl sulfoxide |
| EDTA | ethylenediaminetetraacetic acid |
| EOF | electroosmotic flow |
| GSH | glutathione |
| HPLC | high performance liquid chromatography |
| HV | high-voltage |
| HVPS | high-voltage power supply |
| ISFET | ion selective field effect transistors |
| LC | liquid chromatography |
| LOD | limit of detection |
| LOQ | limit of quantification |
| MAA | mercaptoethanoic acid |
| MCE | microchip capillary electrophoresis |
| 2-MPA | 2-mercaptopropionic acid |
| 3-MPA | 3-mercaptopropionic acid |
| NA-Cys | N-acetyl cysteine |

Abbreviations

| | |
|------------|---|
| NBD-Cl | 4-chloro-7-nitrobenzofurazan |
| PDMS | polydimethylsiloxane |
| PEEK | polyetheretherketone |
| PEG | poly ethylene glycol |
| PMT | photomultiplier tube |
| RSD | relative standard deviation |
| SBD-F | 7-fluorobenzo-2-oxa-1,3-diazole-4-sulfonate |
| SD | standard deviation |
| TTL | transistor-transistor logic |
| μ -TAS | micro total analysis system |
| UV/vis | ultraviolet / visible |

Chapter 1

Introduction

1.1 Introduction and scope

Miniaturization plays a major role in the development of analytical chemistry. As only one example, microfluidic devices were introduced, which handle flows in micrometer-sized channels. Mostly, these structures are integrated into microchips using clean-room technology. Microchip-based methods typically consume less chemicals and require smaller amounts of samples than conventional scale methods do [1]. Furthermore, highly efficient separations in a shorter period of time are achieved as well [2]. Obviously, microfluidic chips are of a small size, and thus many different or parallel processes can be integrated on a single chip [1]. In a broader sense, this miniaturization concept is called micro total analysis system (μ TAS). Many different processes carried out on the microfluidic scale, e.g. on-chip separation, on-chip reaction or on-chip mixing [3].

Since the first published work on microchip capillary electrophoresis (MCE) in 1992 [4, 5] the basic design of CE microchips has almost remained unchanged. Still, MCE has only been scarcely applied to the quantitative analysis of real samples. A suitable MCE system for quantitative analysis

need to allow short analysis times, requires reproducible separations and should be accurate, robust and easy to use. Thus, the goal of this thesis is to investigate the application of MCE to quantitative analysis and to develop analytical methods and instrumentation, which meet the criteria mentioned above. This thesis' chapters cover advances in several different topics of chip-based quantitative analysis.

Chapter 2 gives an overview of the possibilities and limitations for quantitative analysis on a microchip-based capillary electrophoretic system. Theoretical aspects, practical solutions and description of adequate implementation of instrumentation are provided in this chapter. The topics of electrode reactions, buffer decomposition, clogging of microchip channels, surface interactions, adequate power supply, injection and detector-related problems are discussed in this chapter.

The construction of a novel type of high-voltage power supply for microchip capillary electrophoresis is described in chapter 3. This versatile power supply offers all necessary features like the application of high potentials, rapid switching and monitoring of current. A trigger signal can be used for communication of the fully computer-controlled device with external detection systems. The advantage of using high separation potentials for microchip capillary electrophoretic separation is demonstrated by comparing the separation of five analytes carried out applying three different separation voltages.

Two methods were developed to prove the possibility of reproducible and accurate chip-based measurements of real samples. They are described in chapters 4 and 5. MCE is applied to determine thiols in consumer products (chapter 4) and taurine in energy and sports drinks (chapter 5). In both cases, the analytes are derivatized with a fluorogenic reagent to reduce the reactivity of the analyte and to provide sufficient sensitivity for detection. Data validation has been carried out by means of HPLC-fluorescence measurements.

In chapter 6, capillary electrophoretic methods with optical detection are used to determine binding constants of cyclodextrin vesicles with small molecules. α -, β - and γ -cyclodextrin molecules are modified to obtain an amphiphilic character. These amphiphilic molecules form lipid bilayers, which can be transformed into the vesicle state. The affinity of these vesicle hosts towards adamantane carboxylic acid guest molecules will be quantified. The change in electrophoretic mobility, which occurs when binding of the negatively charged guest to the non-ionic vesicles takes place, was measured and used to calculate the respective binding constants.

Chapter 7 concludes this thesis by discussing the results of this work and showing further perspectives of quantitative MCE.

1.2 References

- [1] Whitesides, G. M., *Nature* **2006**, 442, 368-373.
- [2] Janasek, D., Franzke, J., Manz, A., *Nature* **2006**, 442, 374-380.
- [3] Dittrich, P. S., Tachikawa, K., Manz, A., *Anal. Chem.* **2006**, 78, 3887-3907.
- [4] Manz, A., Harrison, D. J., Verpoorte, E. M. J., Fettinger, J. C., Paulus, A., Ludi, H., Widmer, H. M., *J. Chromatogr.* **1992**, 593, 253-258.
- [5] Harrison, D. J., Manz, A., Fan, Z. H., Ludi, H., Widmer, H. M., *Anal. Chem.* **1992**, 64, 1926-1932.

Chapter 2

Microchip Capillary Electrophoresis for Quantitative Analysis[‡]

Obstacles and possible solutions for the application of microchip capillary electrophoresis in quantitative analysis are described and critically discussed. Differences between the phenomena occurring during conventional capillary electrophoresis and microchip based capillary electrophoresis are pointed out, with particular focus on electrolysis, bubble formation, clogging, surface interactions, injection and aspects related to the power supply. Current drawbacks are specified and improvements for successful quantitative microchip capillary electrophoresis are suggested.

[‡] T. Revermann, S. Götz and U. Karst, submitted for publication

2.1 Introduction

Since the introduction of the first analytical device on a chip presented by Terry et al. 1975 [1, 2] the realization of the lab on a chip idea became more and more reality. Progress has been made in creating new microfluidic devices for various applications. Many different designs for chemical reactions, chemical analysis, medical devices and biological applications on a microchip have been published [3-5]. Simple microfluidic constructions were even suggested for undergraduate education [6]. Downscaling of many different detection principles is in progress as well: Classical detection principles like optical methods [7], electrochemical detectors [8] and even mass spectrometers [9-11] are considered as suitable detection systems for lab on a chip devices.

Though the application of capillary electrophoretic separations on microchips has been performed as early as 1992 [12], there has been only little progress regarding quantitative analysis on a microfluidic device. This chapter will review the known examples of quantitative analysis on microfluidic capillary electrophoresis (MCE) devices by means of methods from publications of other scientists and our own work. It will furthermore give an overview about the most crucial aspects, but will also present possibilities to successfully perform this type of analysis on a routine basis in the future.

Generally, separations in micro- or nanoscale dimensions offer the high separation potential of the capillary electrophoretic effect combined with even smaller required amounts of sample and solvents than in conventional CE. It promises rapid and efficient analysis and disposable devices at low costs [13]. The known examples of quantitative analysis on a microfluidic device include inorganic ions, like the determination of nitrite in water [14], calcium in urine [15], lithium in blood [16, 17] and cations as well as anions in tap water [18]. Different organic molecules have been analyzed, for example 4-amino-3-methyl-N-ethyl-N-(β -methane sulfonamidoethyl) aniline in photographic developer [19], oxalate in urine [20], carnitines in water [21], taurine in energy and sport drinks [22], levoglucosan in aerosols [23] and phenols in landfill leachate [24]. The determination of thiols seems to be a topic of special interest, as surprisingly many publications cover this application. The analysis comprises thiols in nerve agent degradation products [25], homocysteine in plasma [26] and thiols in consumer products after derivatization for fluorescence detection [27]. Not only capillary zone electrophoretic (CZE) separations have been published, but isotachopheric approaches are known as well [28, 29]. For some biological and medical applications, a semi-quantitative analysis is sufficient and respective applications for the determination of hepatitis C viruses in serum of clinical patients [30] and DNA in restriction digests of adenovirus 2 [31] have been published.

Our laboratory currently focuses its research on applying microchip capillary electrophoresis (MCE) in analytical and bioanalytical chemistry for quantitative studies in different areas of applications. Another topic is the development of new fluorescence detection systems for microchips, as well as the coupling of chips with a mass spectrometer. In this chapter, the aspects of performing quantitative microchip capillary electrophoresis and the corresponding properties for microchip and detector developments are discussed.

2.2 General aspects for the quantification on microchips – differences of CE and MCE

At a rapid first view, there are little differences between conventional CE and MCE with respect to the separation mechanism and the principles of moving liquids. However, a look at the details reveals several differences, which have practical consequences. The most obvious difference is the type of injection. While conventional CE systems are equipped with a pressure system for hydrodynamic injections, injection of a sample on a microchip is done by electrokinetic methods. This avoids the very difficult task of installing pumps on the microfluidic device and helps to keep the system as simple as possible regarding fabrication. Furthermore, reservoirs installed on the device cannot be moved to and off the separation channel for injection as done in conventional CE. Hydrodynamic injections in analogy to conventional CE are therefore impossible. Injections on microfluidic devices require a new type of injector, which is usually a crossing area of channels, which are connected to four reservoirs. Different types of injections are described in literature [32].

The size of the implemented buffer and sample reservoirs is also different from conventional CE. While discussing the advantages of microfluidics, it is frequently claimed that microchip methodology requires less sample volume and produces less chemical waste than standard instrumentation [33].

Microchips are usually equipped with reservoirs of a volume in the μl range (for example 3 μl [34]). Some researchers attach bigger reservoirs onto the chip separately [24]. However, this approach leads to an increased demand of sample volume.

Another aspect of miniaturization is the separation channel. Comparing the typical dimensions of CE and MCE, it is often observed that the separation path length is reduced rather than its diameter. A slight modification of the geometry of the channel shall not have a major influence on measurement efficiency. The reduction of path length poses the possibility of using higher electric fields, thus inducing more current and heat effects and therefore increased electrolysis.

For the production of microfluidic devices, the implementation of materials other than fused silica / glass is discussed. The application of polymers offers new possibilities with respect to an easier and cheaper manufacturing process [35], but the effects on the performance of analysis have to be considered as well. For this reason surface effects have to be discussed in more detail.

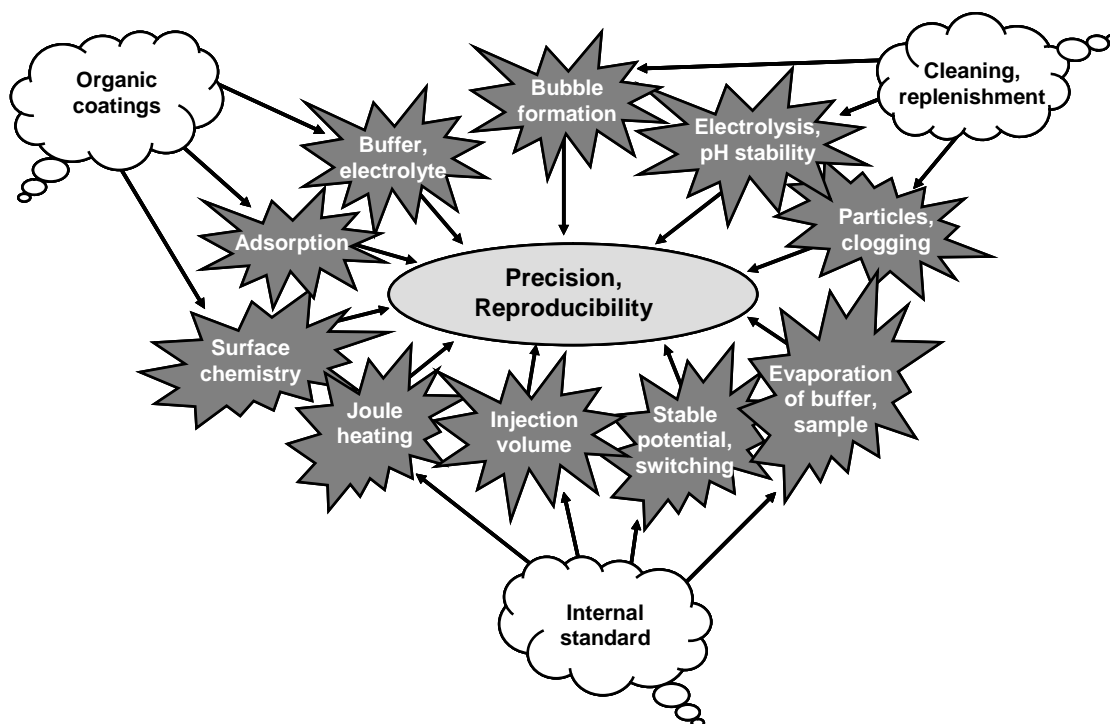


Figure 2.1 Scheme of the influences of different parameters on quantitative Microchip electrophoresis experiments and the respective technical answer.

Quantitative analysis requires optimum reproducibility and accuracy of the measurements and therefore is particularly challenging. Influencing factors and approaches for possible solutions are presented in Figure 2.1. Each group of influencing factors and solutions will be addressed in the following chapters.

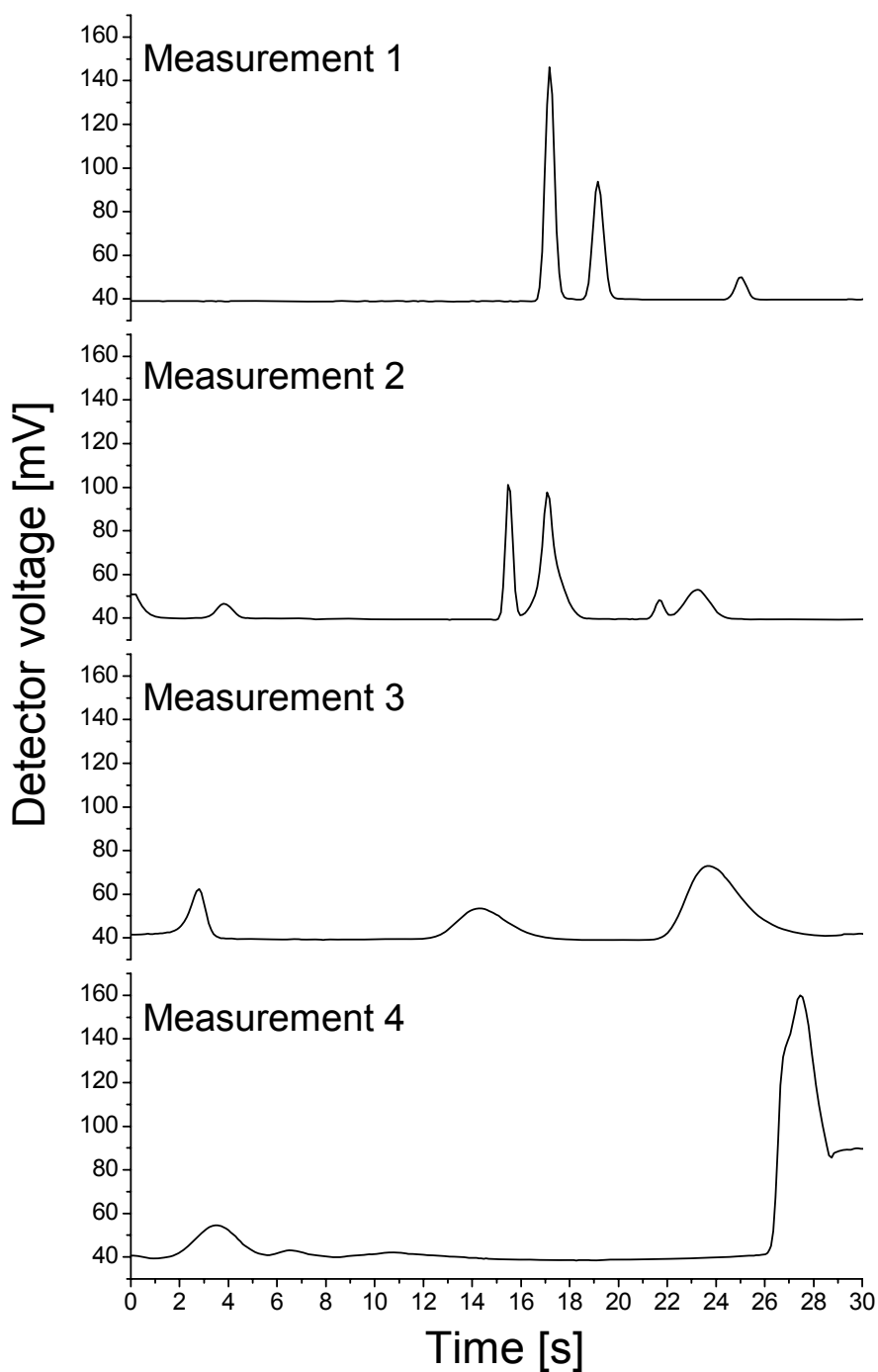


Figure 2.2 A sequence of four measurements on a glass microchip (see Figure 2.3) without replenishing the reservoirs. A separation of three benzo-2-oxa-1,3-diazole-4-sulfonate (SBD) thiol derivatives (Mercaptoethanoic acid, 2- and 3-mercaptopropionic acid, 2 mM each) in a 100 mM sodium citrate buffer pH 4.36 is shown. Voltage program according to Table 2.1.

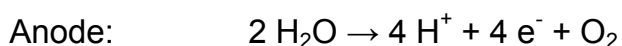
An example how a microchip separation can be influenced after multiple use is shown in Figure 2.2. While an excellent separation is observed for the first injection, the quality of separation deteriorates rapidly with the further injections. Elution times and peak areas change dramatically and additional peaks, which cannot be explained, are occurring. Due to the bad reproducibility of these phenomena starting with the second injection, no routinely used compensation method for these effects is available. Typical phenomena which occur after the first three separations are gases entering the microfluidic channels and the current drops or is highly fluctuating.



Figure 2.3 Scheme of a capillary electrophoresis microchip and applied separation voltages (see Table 2.1). A is buffer inlet, B waste, C outlet and D sample reservoir. Distance from reservoir to injector is 5 mm; the separation channel is 35 mm long. There is a 100 μm offset between channels from reservoir D and B.

2.3 Electrolysis and electrode effects

Electrolysis is maybe one of the biggest problems in MCE. The effect itself is well understood from CE theory, but the consequences for microchip work with its smaller buffer and sample volumes are frequently underestimated. In general, electrolysis will occur and therefore bubbles will be formed. Electrolysis will, however, influence the pH inside the reservoirs. In Figure 2.3, an example of a microchip layout plus the voltages applied during the MCE separation is shown. More data on the voltages applied for loading and separation are available from Table 2.1 [27]. The reactions, which typically take place at the electrodes, are the production of OH^- , H^+ , H_2 and O_2 as described below:



These two reactions are the most prominent ones, but various intermediates or side reaction products with additives or analytes may be formed depending on the particular conditions [36]. For an experiment running 30 s with the separation voltages provided in Table 2.1, the produced amount of H^+ and OH^- can be calculated according to the following example assuming a current I of 100 μA flowing for the time t of 30 s.

$$Q = I \cdot t = 100 \mu\text{A} \cdot 30 \text{ s} = 3000 \mu\text{As} = 3 \text{ mC}$$

$$1 e^- = 1.60217653 \cdot 10^{-19} \text{ C}$$

$$n(e) = 3.109 \cdot 10^{-8} \text{ mol}$$

$$V(\text{res}) = 2.5 \mu\text{L}$$

$$c(\text{H}^+) = \sim 12.4 \text{ mmol/L}$$

Q is the electrical charge; n(e) is the number of electrons. A reservoir content V(res) of 2.5 μl is assumed. One electron has the charge of 1.60217653 · 10⁻¹⁹ C and the Avogadro constant N_A = 6.0221415 · 10²³ mol⁻¹ was used [37].

Table 2.1 Voltage program applied for microchip separations

| | Injection (10s) | separation (30s) |
|------------|-----------------|------------------|
| A (Inlet) | 1800 V | 0 V |
| B (Waste) | 3000 V | 1000 V |
| C (Outlet) | 0 V | 3000 V |
| D (Sample) | 1500 V | 1000 V |

According to the above calculation, an amount of acid (or base) is introduced into the reservoir, which is in the same dimension of the buffering electrolyte concentration. Therefore, pH changes may occur, and separation conditions may change in an unpredictable way. In Table 2.2, the measured pH values

of the reservoir contents are provided after employing the conditions for the analysis of thiols in consumer products according to Table 2.1 and literature [27]. A dramatic change of pH value is measured for the inlet reservoir A, which feeds the separation channel with solution. Thus, the necessity of changing reservoir solutions after every single measurement becomes obvious. Refilling the chip is laborious and time consuming and therefore, many researchers tried to find a more convenient solution which, in addition, also should improve robustness and repeatability of the microchip methodology.

The most obvious solution of the pH problem could be to increase the buffering capacity of the buffer solution by increasing buffer capacity. However, the resulting increase in conductivity leads to an increased current and therefore increased electrolysis, which compensates for this effect. The required calculations have been performed by Bello [38].

Table 2.2 pH values measured by pH indicator strips of the reservoir content of a standard microchip after one and three measurements. Applied voltages according to Table 2.1. All four reservoirs were filled with 2.5 μ L citrate buffer, 100 mM pH 4.36.

| Reservoir | pH after | |
|------------|----------|----------|
| | 1 cycle | 3 cycles |
| A (Inlet) | 5-6 | 13-14 |
| B (Waste) | 3-4 | 3 |
| C (Outlet) | 4 | 3-4 |
| D (Sample) | 4 | 4 |

Some researchers attach additional reservoirs onto the microchip to increase the reservoirs in size. This should, at the first sight, lead to a decreased effect of electrolysis due to the dilution of the electrolysis products in a larger buffer volume. However, there are three disadvantages associated with this strategy: First, the reservoirs have to be attached manually in a laborious procedure to any individual microchip. Second, it leads to the demand for an increased sample volume, thus spoiling one of the most important arguments for microchip CE, the need for extremely small samples volumes. Conventional CE instruments can be run with about 500 μl buffer per vial and starting with 10 μl of sample which can be used for multiple injections, though techniques to inject even submicroliter volumes are also known [39]. Finally, diffusion in the enlarged reservoirs may be so slow that there is no complete and rapid mixing between the lower part, in which the electrodes are located (particularly in those cases, where the electrodes are manufactured on-chip) and the upper part of the reservoir. This may become the cause of further reproducibility problems.

Another possible solution would be the opposite approach, which is the use of electrolytes with low intrinsic conductivities like bigger organic molecules and buffer solutions, in which both anion and responding cation have buffering abilities. These buffers are also called “Good” or “Good-type buffers” [40]. However, there are additional requirements for a buffer in CE as matching the mobility of analyte and buffer ion for example and the

suitability of these buffers will have to be tested individually.

In literature, other approaches to overcome the problems of buffer electrolysis are reported as well. As electrolysis may also take place for conventional CE, different solution strategies have been developed for this technique. De Jesus et al. added external compartments for electrolysis to the CE equipment. No significant changes in migration time and resolution were observed for 15 runs on a conventional CE equipment [41]. Despite its usefulness, however, this approach adds complexity to the analytical system and is therefore not likely to be adapted on a large scale. Even in conventional CE, positioning of electrodes is an important parameter with which the introduction of alkaline or acid products of the electrodes into the capillary can be minimized [42]. A pH monitoring system for small buffer volumes in conventional CE was presented by Timperman et al. [43]. Systems for continuous replacement of buffer [44] or single use of CE vials were suggested [45]. To reduce the electrical current especially for separations with high electric fields, the use of zwitterionic buffers with low conductivity properties is advised [46, 47]. The choice of Good-type buffers and buffer capacity as well as ionic strength is summarized by Reijenga et al. [48]. whereas Kelly et al. described approaches to reduce the buffer electrolysis in pharmaceutical analysis [49]. Fuller and Sweedler described the injection of submicroliter volumes into the CE system and the occurring problems. Samples were injected electrokinetically and an internal standard was used for correction of the data. The detection of electrochemically generated species and therefore the dependency of the electrode-to-channel

distance are presented [39]. Problems described in this chapter are therefore also relevant for chip based techniques due to the small sample volumes and the small distances between electrodes and capillary.

Some more recent research focuses on the effects in microfluidic channels. Oki et al. measured the pH inside microchannels by ion-selective field effect transistors (ISFETs). They neutralized upcoming pH differences by electroosmotic flow (EOF)-pumped counter titration and included, in a different experiment, salt bridges to prevent the introduction of alkaline and acidic solutions into the separation channel [50].

Pressure effects on microchips are described by Crabtree et al. [51]. Natural pH gradients can be generated in microfluidic channels and used for isoelectric focusing [52]. Approaches to quantify and evaluate Joule heating in MCE systems using as much as 1500 V cm^{-1} are described [53]. The dependency of the chip design on peak broadening in MCE was evaluated by Gas and Kenndler [54]. Lin et al. developed a microchip with a waste removing function and automated sample reloading, channel washing and reconditioning. They applied an internal standard and claimed that their system is suited for quantitative analysis. This complex microfluidic system was only used for gated injection [55].

2.4 Bubble formation and particles

As these two effects may be overcome by similar strategies, they are discussed together within this chapter. Bubble formation is a result of the electrolysis taking place during an electrophoretic run and therefore can only be reduced, but not abolished. Nevertheless, it is well possible to vary the position of electrodes and geometry of buffer reservoirs to minimize bubble formation. It is necessary to place the electrodes not too far away from the channel outlet, but gas should not enter the microfluidic channels.

The usual location, where particles and gas bubbles clog channels is the injector. Due to its geometry, particles (dust, fibers from tissues etc.) tend to block the channels there. A straight capillary usually offers no foothold, in which macroscopic materials can stick during flushing steps.

Particles and gas from buffers can be removed by filtration of all used solutions. If solutions are stored in closed containers and only fresh solutions are used, a clogging event is reasonably rare so that microchips can be used in a conventional chemistry laboratory without any clean room atmosphere. Local degassing due to pressure differences should be avoided anyway, as hydrodynamic pressures deteriorate the separation efficiency in CE.

Monitoring the current always provides valuable information about the status of the experiment. Reproducible and stable currents are a reliable hint for successful separations, as a sudden decrease of current combined with a higher fluctuation of current indicates that a bubble or a particle has entered the microfluidic channels. The only consequence in those cases is to flush the chip thoroughly and to refill the reservoirs.

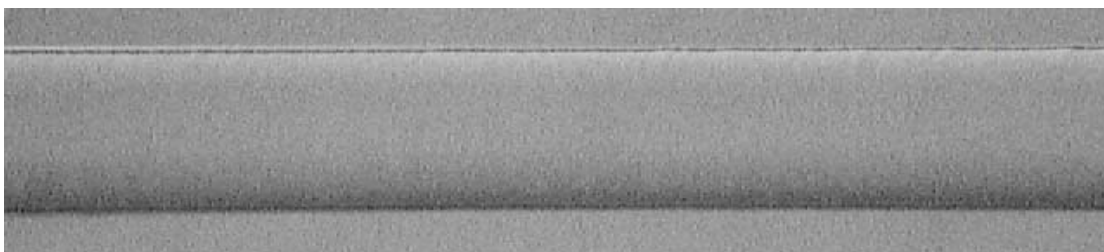
2.5 Surface interactions and materials

Surface chemistry poses a challenge to the analytical chemist in capillary electrophoresis, as many analytes or sample constituents interact with the capillary walls, which are essential for CE separations. The effect of analyte adsorption on the EOF in microfluidic channels is reported by Ghosal [56]. Prominent examples are protein and DNA separations [57]. This factor counts in the same way for MCE as for CE with the addition that in MCE, other materials than glasses are used as well. Microchips made from polymer materials are advantageous over glass chips during the manufacturing process. For the production of every single glass microchip, clean room equipment is necessary. Most polymer-based substrates ask for a clean room-manufactured stamp, which is used to reproduce a manifold of microchips outside the clean room environment. Commonly used polymers for microchip separations are PDMS [58] or commodity polymers [35, 59]. Combinations of different channel wall materials are prone to create an inhomogeneous EOF if no special coating is used. In principle, all coating materials, which are used in conventional CE capillaries, may be applied for microchip CE as well, although the transfer to glass substrates should be easiest because of the similarity to the fused silica material of conventional capillaries. The purpose of applying coatings to modify the properties of the capillary / channel surface is the reduction or elimination of analyte-surface interaction, thus improving reproducibility, resolution and / or separation speed. The applied coating will reverse, abolish or change the EOF to a less

pH dependent value [60]. Some coatings are applied permanently; others demand just an addition to the running electrolyte. These coatings may therefore be a valuable tool for MCE separations [61].

A smooth surface of the channels is desired for efficient and reproducible MCE separations. The comparison of HF-etched and powder-blasted glass microchips yielded higher separation efficiencies for the HF etching. Etched surfaces had a roughness of 3-15 nm, whereas powder-blasted surfaces were in the range of 1-5 μm [62]. Figure 2.4 shows pictures of a new and a used micro channel. The surface in the used channel was probably damaged by an electrical discharge. The resulting higher surface roughness might have an influence on the measurements. Therefore the use of such channels as separation channels should be avoided if high separation efficiencies are desired. However, according to our experience, glass microchips can be reused even many hundred times in case of proper use and surface treatment.

unused channel



damaged channels

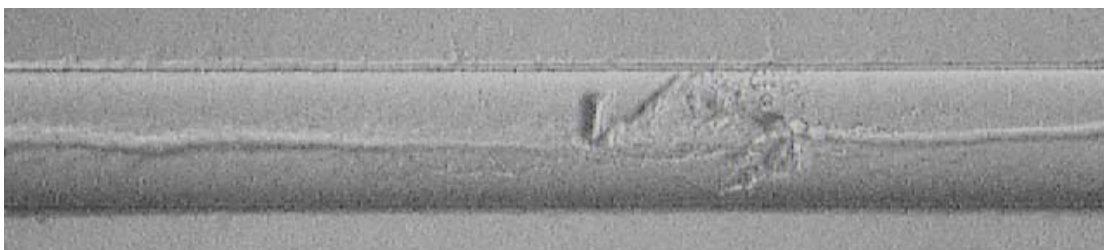
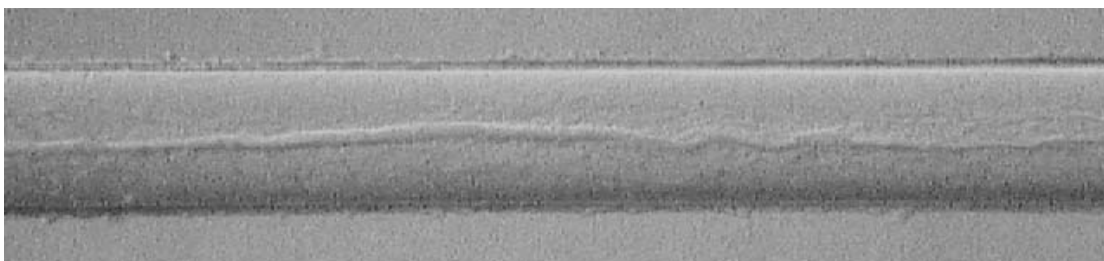


Figure 2.4 Pictures of an unused channel and of damaged channels in glass microchips

2.6 Injection and Power supply

As MCE is a relatively new technique, instrumentation is not as mature as in conventional CE. Furthermore, the requirements for a MCE high-voltage power supply are much more complex than in conventional CE, where only one high-voltage power supply with sufficient specifications with respect to voltage, maximum current and stability is needed. In MCE, four independent electrodes have to be controlled in the kV range and switched within milliseconds from injection to separation mode. This switching is technically demanding, because either high-voltage relays or voltage sources with short adjusting times are required. To our experience, there is no single power supply on the market, which can cope with the demands for a voltage of at least 5 kV at four channels, a current of approximately 1 mA, the possibility to monitor voltage and current on all channels, a switching time in the low millisecond time and a user-friendly software control of the instrument.

2.7 Detector related problems

While developing a fluorescence detection system in the lab [63], several parameters which have to be considered before construction of the detector were encountered. In general, these problems are specific to optical methods, as they concern detection volume, distance to the injector and proper alignment of the microchip inside the chip holder. To replenish all reservoirs frequently as suggested above, the chip has to be removed from the holder and re-aligned after replenishment. Depending on the objective used, the adjustment in the orthogonal direction of the channel has to be done on the micrometer scale. If a channel of 50 μm width is magnified by a 60 fold objective the visible spot is about 150 μm in diameter, which means that a displacement of 50 μm will move the detection volume out of focus. Thus positioning of the microchip has to be done in the μm range.

Generally, the objective determines the detection volume, which has furthermore an influence on the efficiency of the separation. Higher intensities through monitoring a larger section with an objective with less magnification results in losing resolution, as the detector requires the peaks to be fully out of the observed section. This happens although the human eye could also discriminate between two baseline-separated peaks in the observed section because of its spatially resolved detection.

An effect, which is only observed during optical detection, is that measuring fluorescent peaks deteriorates separation efficiency. The wavelengths are selected in such a way that analyte molecules absorb the light. As this energy is transferred to the analytes, these are locally heated, which increases diffusion. Therefore, for optimum separations, it is not recommended to illuminate the whole chip or to follow the injected plug optically to monitor the separation.

2.8 Problem solving in MCE

In analytical chemistry, internal standards are often used to correct for various experimental errors [39, 64, 65]. An internal standard is a substance, which behaves as similar as possible compared to the analyte. There are many different approaches to use an internal standard, which cannot be discussed in detail at this point. However, internal standards may also be a valuable tool for quantitative MCE: An internal standard was used by a group of authors [22, 27] not only to correct for reaction yields but also to adjust MCE results for detector alignment, reproducibility of injection volume and migration time. Changes in EOF and therefore speed of the separation do have an influence on the detected signal if non-destructive detectors are used. In this case, the analyte stays within the detection window for a longer time. Concentration changes due to solvent evaporation and different optical alignment in the detector can be also corrected by this approach.

Our research group utilizes glass microchips without on-chip electrodes. An in-house built chip holder is equipped with platinum electrodes fixed inside a polymer block with adjusted distances to address each reservoir on the microchip equally. This way, electrodes are placed from the top into the middle of the reservoir, having the electrode close enough to the capillary openings and still contacting the reservoir content with a relatively high surface compared to on-chip electrodes. The electrode blocks provide an extra bore which, when sealed with o-rings, can be used as an additional reservoir volume. Nevertheless, MCE may also be operated using the on-chip reservoir only, thus resulting in rapid and easy handling.

2.9 Future challenges and opportunities

When considering the aspects indicated above, there is now a solid basis of knowledge and techniques available for quantitative microchip capillary electrophoresis with excellent and reproducible results. We believe that there are no fundamental constraints, which cannot be solved for downscaling CE to MCE for quantitative analysis. Nevertheless, at this point of development, operators have to create their microchip-based separations with even more care than done with conventional CE methods. Advances in instrumentation and gathered experience while working with quantitative MCE will propel the broader application of MCE in analytical chemistry. The full benefits of microchip technology will be gained when for example derivatization reactions are integrated on chip, which will definitely save labor and will effectively reduce analysis times. What is still missing at this point? Still, there are no universal autosampler systems available, which would allow rapid and reproducible injection, an operation of a MCE system on a 24/7 base and the use of many different separation programs as is nowadays routine in established analytical separation systems. It is difficult to argue for the extremely rapid separations in MCE, when the replenishment of buffers by hand consumes at least the tenfold time of the separation itself. It can be expected that the transfer of quantitative MCE from a limited number of research labs into broad industrial application will strongly depend on the availability of automated and reliable instrumentation for quantitative MCE with high sample throughput, which address these aspects in a proper way.

2.10 References

- [1] Terry, S. C., *Ph.D. Dissertation*, Stanford University, **1975**.
- [2] Terry, S. C., Jerman, J. H., Angell, J. B., **1979**, *ED-26*, 1880-1886.
- [3] Reyes, D. R., Iossifidis, D., Auroux, P. A., Manz, A., *Anal. Chem.* **2002**, *74*, 2623-2636.
- [4] Auroux, P. A., Iossifidis, D., Reyes, D. R., Manz, A., *Anal. Chem.* **2002**, *74*, 2637-2652.
- [5] Dittrich, P. S., Tachikawa, K., Manz, A., *Anal. Chem.* **2006**, *78*, 3887-3907.
- [6] Almaraz, R. T., Kochis, M., *J. chem. edu.* **2003**, *80*, 316-319.
- [7] Götz, S., Karst, U., *Anal. Bioanal. Chem.* **2007**, *387*, 183-192.
- [8] Vandaveer, W. R., Pasas-Farmer, S. A., Fischer, D. J., Frankenfeld, C. N., Lunte, S. M., *Electrophoresis* **2004**, *25*, 3528-3549.
- [9] Uchiyama, K., Nakajima, H., Hobo, T., *Anal. Bioanal. Chem.* **2004**, *379*, 375-382.
- [10] Schwarz, M. A., Hauser, P. C., *Lab Chip* **2001**, *1*, 1-6.
- [11] Mogensen, K. B., Klank, H., Kutter, J. P., *Electrophoresis* **2004**, *25*, 3498-3512.
- [12] Manz, A., Harrison, D. J., Verpoorte, E. M. J., Fettinger, J. C., Paulus, A., Ludi, H., Widmer, H. M., *J. Chromatogr.* **1992**, *593*, 253-258.
- [13] Janasek, D., Franzke, J., Manz, A., *Nature* **2006**, *442*, 374-380.

- [14] Greenway, G. M., Haswell, S. J., Petsul, P. H., *Anal. Chim. Acta* **1999**, 387, 1-10.
- [15] Malcik, N., Ferrance, J. P., Landers, J. P., Caglar, P., *Sens. Actuator B-Chem.* **2005**, 107, 24-31.
- [16] Vrouwe, E. X., Luttge, R., van den Berg, A., *Electrophoresis* **2004**, 25, 1660-1667.
- [17] Vrouwe, E. X., Luttge, R., Olthuis, W., van den Berg, A., *Electrophoresis* **2005**, 26, 3032-3042.
- [18] Vrouwe, E. X., Luttge, R., Olthuis, W., van den Berg, A., *J. Chromatogr. A* **2006**, 1102, 287-293.
- [19] Sirichai, S., de Mello, A. J., *Analyst* **1999**, 125, 133-137.
- [20] Zuborova, M., Masar, M., Kaniansky, D., Johnck, M., Stanislawski, B., *Electrophoresis* **2002**, 23, 774-781.
- [21] Kameoka, J., Craighead, H. G., Zhang, H. W., Henion, J., *Anal. Chem.* **2001**, 73, 1935-1941.
- [22] Götz, S., Revermann, T., Karst, U., *Lab Chip* **2007**, 7, 93-97.
- [23] Garcia, C. D., Engling, G., Herckes, P., Collett, J. L., Henry, C. S., *Environ. Sci. Technol.* **2005**, 39, 618-623.
- [24] Wu, Y. Y., Lin, J. M., *J. Sep. Sci.* **2006**, 29, 137-143.
- [25] Wang, J., Zima, J., Lawrence, N. S., Chatrathi, M. P., Mulchandani, A., Collins, G. E., *Anal. Chem.* **2004**, 76, 4721-4726.
- [26] Pasas, S. A., Lacher, N. A., Davies, M. I., Lunte, S. M., *Electrophoresis* **2002**, 23, 759-766.

- [27] Revermann, T., Götz, S., Karst, U., *Electrophoresis* **2007**, *accepted for publication*.
- [28] Masar, M., Zuborova, M., Bielcikova, J., Kaniansky, D., Johnck, M., Stanislawski, B., *J. Chromatogr. A* **2001**, *916*, 101-111.
- [29] Bodor, R., Madajova, V., Kaniansky, D., Masar, M., Johnck, M., Stanislawski, B., *J. Chromatogr. A* **2001**, *916*, 155-165.
- [30] Young, K. C., Lien, H. M., Lin, C. C., Chang, T. T., Lee, G. B., Chen, S. H., *Talanta* **2002**, *56*, 323-330.
- [31] Mueller, O., Hahnenberger, K., Dittmann, M., Yee, H., Dubrow, R., Nagle, R., Ilsley, D., *Electrophoresis* **2000**, *21*, 128-134.
- [32] Wenclawiak, B. W., Puschl, R., *Anal. Lett.* **2006**, *39*, 3-16.
- [33] Whitesides, G. M., *Nature* **2006**, *442*, 368-373.
- [34] Zhang, C. X., Manz, A., *Anal. Chem.* **2001**, *73*, 2656-2662.
- [35] Becker, H., Locascio, L. E., *Talanta* **2002**, *56*, 267-287.
- [36] Corstjens, H., Billiet, H. A. H., Frank, J., Luyben, K., *Electrophoresis* **1996**, *17*, 137-143.
- [37] Lide, D. R., *Handbook of Chemistry and Physics*, CRC Press, Boca Raton **2004**.
- [38] Bello, M. S., *J. Chromatogr. A* **1996**, *744*, 81-91.
- [39] Fuller, R. R., Sweedler, J. V., *Anal. Chem.* **1999**, *71*, 4014-4022.
- [40] Good, N. E., Winget, g. D., Winter, W., Connolly, T. N., Izawa, S., Singh, R. M. M., **1966**, *5*, 467-477.

- [41] de Jesus, D. P., Brito-Neto, J. G. A., Richter, E. M., Angnes, L., Gutz, I. G. R., do Lago, C. L., *Anal. Chem.* **2005**, *77*, 607-614.
- [42] Macka, M., Andersson, P., Haddad, P. R., *Anal. Chem.* **1998**, *70*, 743-749.
- [43] Timperman, A., Tracht, S. E., Sweedler, J. V., *Anal. Chem.* **1996**, *68*, 2693-2698.
- [44] Carson, S., Cohen, A. S., Belenkii, A., Ruizmartinez, M. C., Berka, J., Karger, B. L., *Anal. Chem.* **1993**, *65*, 3219-3226.
- [45] Zhang, C. X., Thormann, W., *Anal. Chem.* **1996**, *68*, 2523-2532.
- [46] Stoyanov, A. V., Pawliszyn, J., *Analyst* **2004**, *129*, 979-982.
- [47] Hjerten, S., Valtcheva, L., Elenbring, K., Liao, J. L., *Electrophoresis* **1995**, *16*, 584-594.
- [48] Reijenga, J. C., Verheggen, T., Martens, J., Everaerts, F. M., *J. Chromatogr. A* **1996**, *744*, 147-153.
- [49] Kelly, M. A., Altria, K. D., Clark, B. J., *J. Chromatogr. A* **1997**, *768*, 73-80.
- [50] Oki, A., Takamura, Y., Ito, Y., Horiike, Y., *Electrophoresis* **2002**, *23*, 2860-2864.
- [51] Crabtree, H. J., Cheong, E. C. S., Tilroe, D. A., Backhouse, C. J., *Anal. Chem.* **2001**, *73*, 4079-4086.
- [52] Macounova, K., Cabrera, C. R., Holl, M. R., Yager, P., *Anal. Chem.* **2000**, *72*, 3745-3751.
- [53] Swinney, K., Bornhop, D. J., *Electrophoresis* **2002**, *23*, 613-620.
- [54] Gas, B., Kenndler, E., *Electrophoresis* **2002**, *23*, 3817-3826.

- [55] Lin, C.-C., Chen, C.-C., Lin, C.-E., Chen, S.-H., **2004**, *1051*, 69-74.
- [56] Ghosal, S., *Anal. Chem.* **2002**, *74*, 771-775.
- [57] Doherty, E. A. S., Meagher, R. J., Albarghouthi, M. N., Barron, A. E., *Electrophoresis* **2003**, *24*, 34-54.
- [58] McDonald, J. C., Duffy, D. C., Anderson, J. R., Chiu, D. T., Wu, H. K., Schueller, O. J. A., Whitesides, G. M., *Electrophoresis* **2000**, *21*, 27-40.
- [59] Becker, H., Gartner, C., *Electrophoresis* **2000**, *21*, 12-26.
- [60] Horvath, J., Dolník, V., **2001**, *22*, 644.
- [61] Belder, D., Ludwig, M., *Electrophoresis* **2003**, *24*, 3595-3606.
- [62] Pu, Q.-S., Luttge, R., Gardeniers, H. J. G. E., van den Berg, A., **2003**, *24*, 162-171.
- [63] Götz, S., Karst, U., *Sens. Actuator B-Chem.* **2007**, *in press*, DOI:10.1016/j.snb.2006.1008.1027.
- [64] Dose, E. V., Guiochon, G. A., *Anal. Chem.* **1991**, *63*, 1154-1158.
- [65] Oates, M. D., Cooper, B. R., Jorgenson, J. W., *Anal. Chem.* **1990**, *62*, 1573-1577.

Chapter 3

Extendable four channel high-voltage power supply for fast microchip capillary electrophoretic separations[‡]

The construction and application of a four channel high-voltage power supply for chip-based capillary electrophoretic analysis is described. The presented design, without any electronic components in the high-voltage path, offers the advantages of a voltage of 6kV per channel, a maximum current of 1 mA and the option of application-specific upgrading the instrument to even higher voltages and currents by changing one or more high-voltage modules without limitations. The use of four independent high-voltage outputs allows the use of standard as well as specially designed chips and different injection techniques. The fully computer-controlled instrument switches in less than 50 ms from 0 to 6 kV for optimum control of the injection and separation step. The separation of five derivatized thiols was used to demonstrate the advantages of using high-separation potentials at high currents to achieve very rapid analysis.

[‡]M. Kießhauer, T. Revermann, J. Künnemeyer and Uwe Karst, submitted for publication

3.1 Introduction

Miniaturized total analysis systems offer a large variety of new possibilities in chemical and biochemical analysis [1]. Chip-based capillary electrophoretic methods require high quality power supplies for reproducible analyses. Especially when aiming at quantitative analysis [2], a power supply is required, which offers sufficiently high voltages to ensure quick separations, allows currents of a reasonable height and guarantees fast switching between different voltages to change the potentials from injection to separation mode. In contrast to conventional capillary electrophoresis (CE), four electrodes and therefore four potentials have to be controlled and their voltage has to be switched in a fast and reproducible way in microchip capillary electrophoresis (MCE). Since the first presented analytical device using capillary electrophoresis as a separation mechanism on a microfluidic device [3, 4], research focused on the development of new structures and manufacturing processes for microchips [5]. The development of high-voltage power supplies (HVPS) focused on, according to literature, minimizing the number of voltage sources [6, 7] or developing portable high-voltage (HV) units [8-10] for field measurements. Some of the described instruments are therefore battery powered [8-11].

Table 3.1: Comparison of different power supplies. nr: not reported; g: ground;

*after adjusting time of 10s per channel; **our measurements showed 44 ms.

| | V max. [kV] | I max. [μ A] | Switching time [ms] | voltage outputs (different voltages) | current monitor | limited to special microchip / injection | battery / line powered | number and type of HV sources |
|---------------------|----------------|----------------------|---------------------------|--|--------------------|--|------------------------------|----------------------------------|
| novel HVPS | 6 | 1000 | <50 ms | 4 (4) | yes | no | line | 4 pos. + 1 neg. |
| Caplix | 2 | 100 | 10 ms** | 4 (4) | yes | no | line | 4 pos. + 1 neg. |
| Micronit | 3 | 1000 | 4* | 8 (8) | yes | no | line | 8 pos. + ground |
| Jacobson et al. [7] | 1.1 | nr | nr | 2 (1) | nr | yes | line | 1 + ground |
| Garcia et al. [11] | ± 4 | nr | 20 ms | 4 (3) | nr | pinched + gated | both | 2 pos. + 1 neg. + g |
| Jackson et al. [9] | 0.87 / 1.36 | 380 | nr | 4 (2) | nr | pinched | battery | 2 + diodes and resistors |
| Collins et al. [6] | 15 | 260 | nr | 4 (3 + g) | yes | gated | line | voltage divider network |
| Erickson et al. [8] | 0.7 | nr | nr | 3 (3) | nr | yes | battery | 1 + resistors |
| Renzi et al. [10] | ± 5 | 100 | 20 ms | nr | yes | yes | battery | 12 bivalent |

However, there are only few commercial power supplies on the market, and the currently available commercial instrumentation does not fulfill the requirements a modern lab-on-a-chip approach has. Most power supplies allow only insufficiently high-voltages of 4 kV or, in most cases, less [6]. This counts for many commercial products as well as instrumentation described in the scientific literature [7-9]. An overview over the specifications of nine different instruments is provided in Table 3.1. In this chapter, a novel design of HVPS is described, which allows an easy, application-specific upgrade to different voltages without changing the structure of the instrument itself. In its current form, the maximum voltage per channel is 6 kV and the maximum current is 1 mA. The presented instrument is fully computer-controlled and can be used in conjunction with various chip designs and types of injection, as it is equipped with four independent high-voltage channels. The use of high separation potentials is demonstrated by the separation of five derivatized thiols.

3.2 Experimental

3.2.1 Electronic components

The most essential electrical components for the construction of the HVPS include the following parts: MF 60/5 steel chassis 350 x 270 x 95 mm (Metal Forums Engineering); S6-6p-L12HV-modules 0-6 kV 1 mA regul. chassis L12 & CN8R option (Hivolt); F80 HV-module 0.37-8kV 1.23 mA +/- I/O-Prob PCB (Hivolt); switching power supply LPT 43 (Traco Powers); switching power supply TXL150-24 (Astec); labjacks U12, USB (Meilhaus); high-voltage resistors HTS523, 1 W, 10 M Ω ; reed relay dip 7212 – L 5 V; power line filter Schaffner FN 284-6/06; IC OP495 GP; LED SLH 56 WS, 5 mm, super bright, clear, white; printed circuit board 160 x 100 mm and 200 x 200 mm, 1.5 mm, 35 μ m; male and female high-voltage coaxial connectors SHV series 12 kV 10A 50 Ω (Radial); G6C – 111 7 P-US relays (Omron); octal driver array ULN 2803. MS Visual basic 2005, MS Excel 2003 and SQL server were used as software packages (all Microsoft).

3.2.2 Chemicals, microchips and detection system

A 50 mM borate buffer at pH 9.50 containing 5 mM of EDTA was used for the reaction of thiols with ammonium-7-fluorobenzo-2-oxa-1,3-diazole-4-sulfonate (SBD-F). The test sample contains mercaptoethanoic acid (MAA), 2-mercaptopropionic acid (2-MPA), N-acetylcysteine (NA-Cys), 3-mercaptopropionic acid (3-MPA) and reduced glutathione (GSH) in a concentration before derivatization of 0.5, 1, 10, 10 and 5 mmol L⁻¹. MCE separations were performed with a 50 mM citrate buffer at a pH of 4.36. Detailed synthesis, preparation and derivatization procedures are described in a previous publication [12].

Glass microchips for MCE, model T3550 were obtained from Micronit Microfluidics with a channel width of 50 µm and a depth of 20 µm. A channel of 5 mm length transports buffer or sample solutions into the injector. The separation path length is 35 mm with 27 mm from the double tee injector to the position of the detection volume. The microchip is positioned inside an in-house built chip holder containing platinum wires as electrodes. Chips were flushed with a 500 µl syringe (SGE) equipped with a Teflon liner (Upchurch Scientific) and all reservoirs were refilled with 3.0 µl solution prior to each measurement.

A fluorescence microscope-based setup was used as a detector, consisting of an inverse IX-71S1F fluorescence microscope (Olympus) and an Olympus xenon burner (U-LH75XEAP0). Wavelength selection was performed by a filter cube with components from Chroma (exciter: D390/70X 104733; dichroic: 440DCXR; emitter: HQ500LP 47767). Signals were detected by a Hamamatsu H5784 photomultiplier tube and recorded at 50 Hz by McDACq software (Bischoff). Integration and calculation of parameters shown in Table 3.3 were performed with Dax Data Acquisition v. 6.0 (Prince Technologies).

Measurements of output voltage of the instrument were performed on a Tektronix TDS 210 instrument with 2.5 kV detector probes and Open Choice Desktop software version 1.10 (Tektronix). As this setup can only stand voltages up to 4 kV, the output channel voltage (6 kV) was measured with an additional voltage divider and calculated back to the original voltage, which reduces precision and increases noise.

3.3 Results and Discussion

3.3.1 Construction of the HVPS

Four programmable high-voltage units are the core of the instrument. They are equipped with an internal voltage and current monitoring system and can be adjusted to another voltage from 0 to 6 kV in less than 50 ms. A schematic wiring diagram of a voltage module is given in Figure 3.1. The HV units are connected directly to the output of the channel. On the input side, the 24 V feed voltage can be switched by relays. Setting voltages and timing of relays as well as reading out monitoring channels is performed via two Labjack controller boards, which can be connected via USB ports to a conventional computer without installing additional hardware. A wiring scheme of the HVPS instrument is given in Figure 3.2.

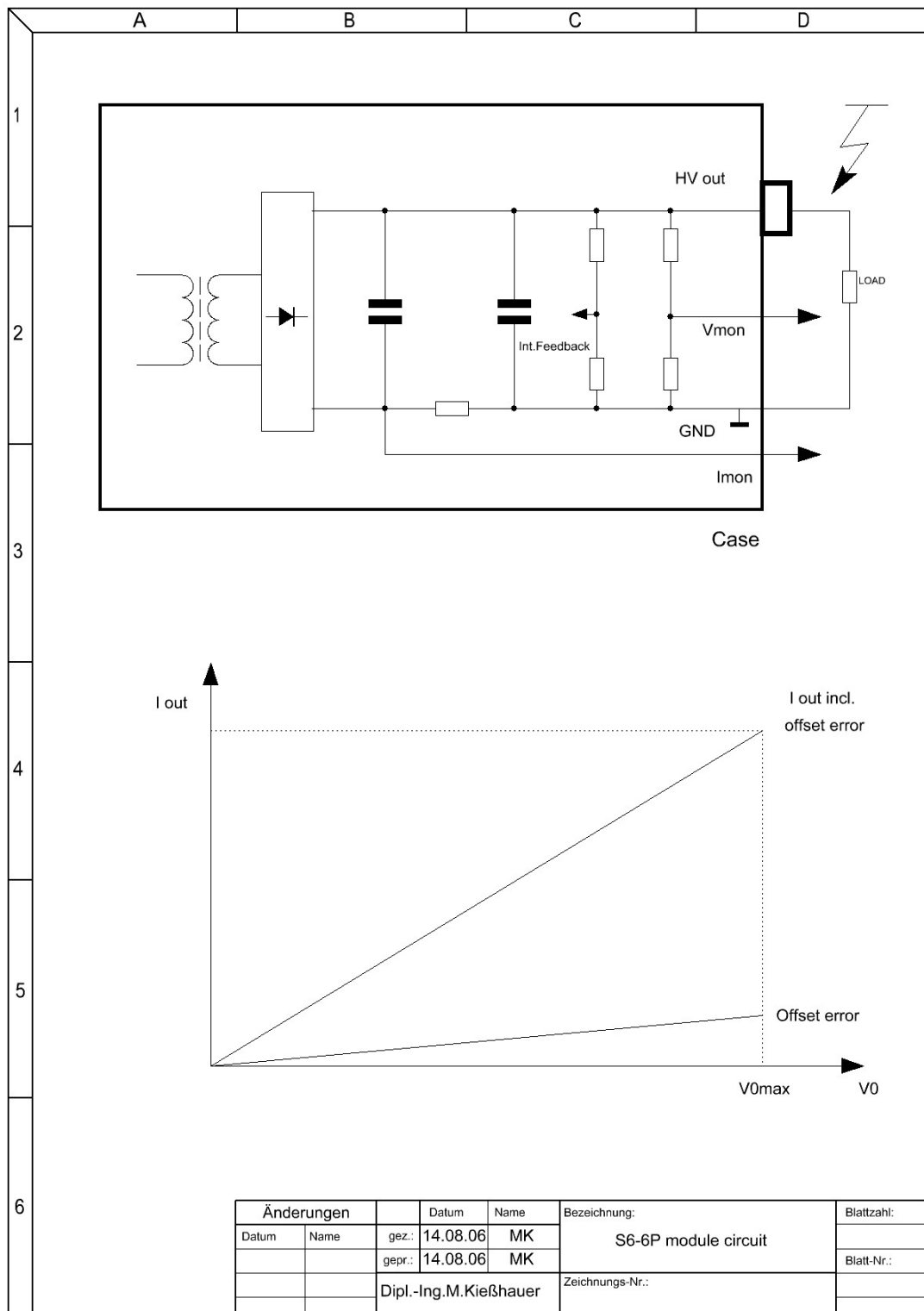


Figure 3.1: Schematic diagram of a high voltage module including current and voltage monitoring channels and offset errors.

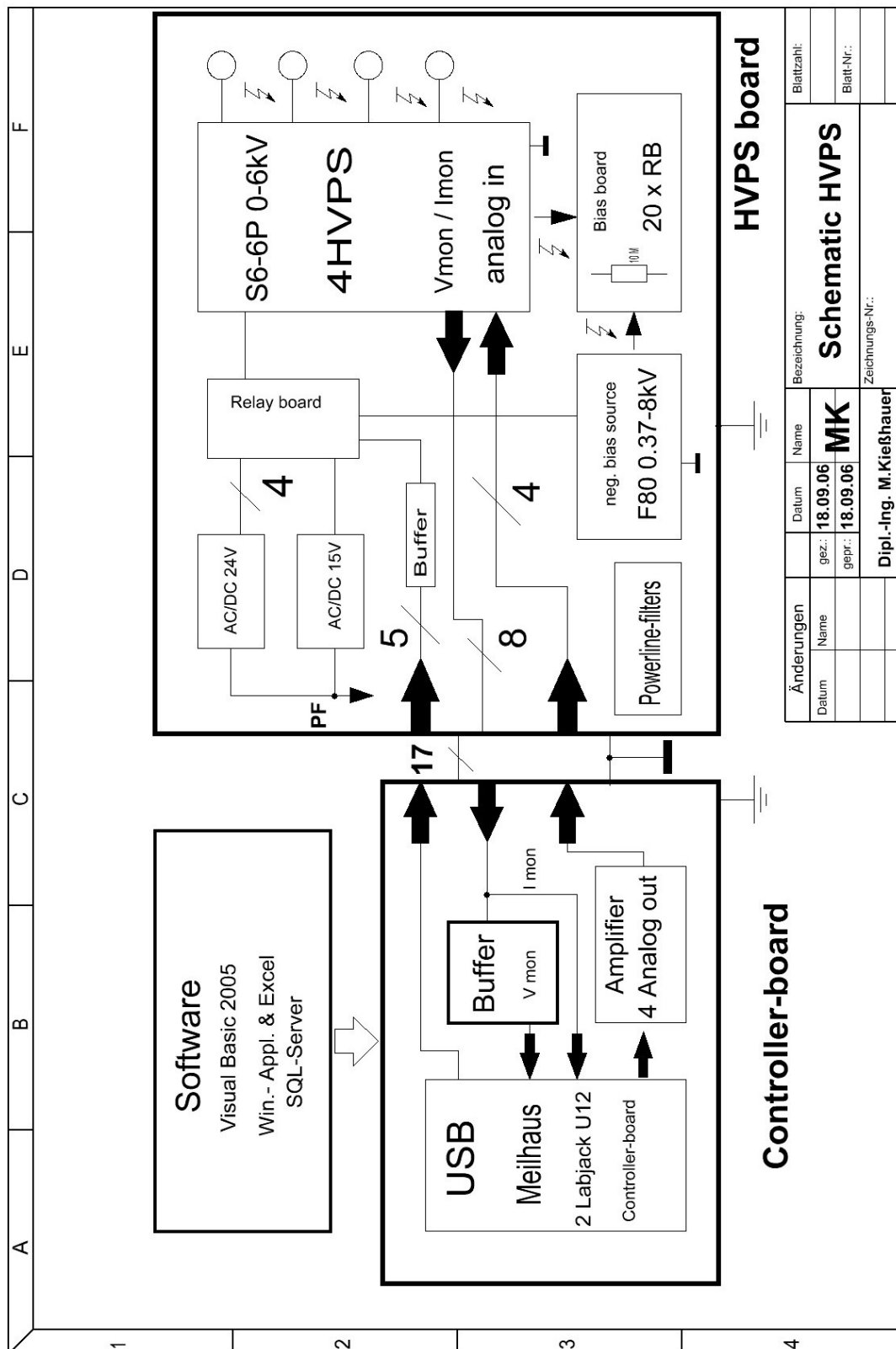


Figure 3.2: Schematic wiring diagram of the HVPS.

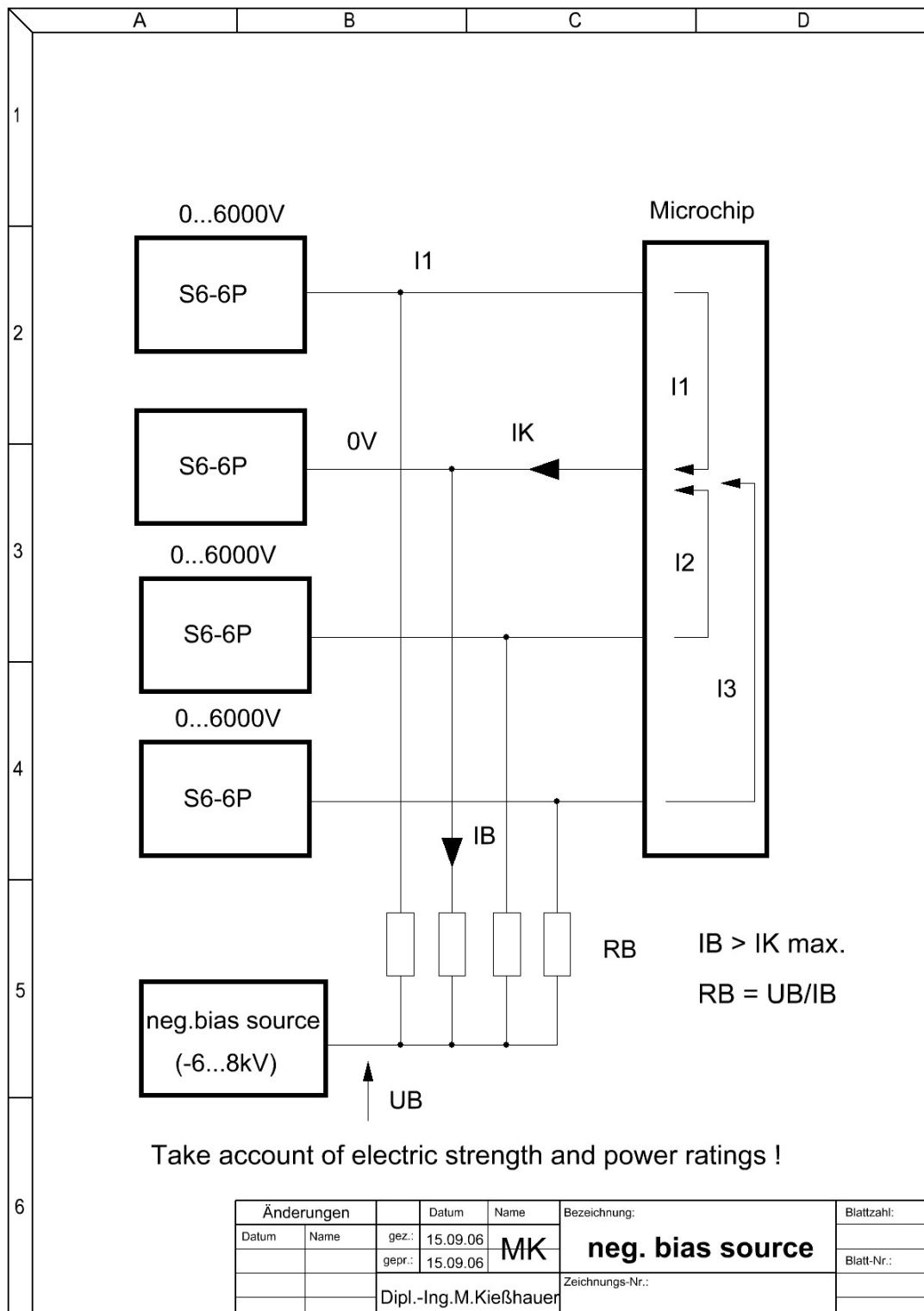


Figure 3.3: Schematic wiring diagram of the connections to the negative bias high voltage unit.

All four HV units are of positive nature and deliver currents, thus requiring a current sink as well. A negative bias HV unit fulfils this task when connected via HV resistors to each of the output channels. This offers all positive HV units to deliver their current, even if a potential is set to zero, which represents ground in most other devices. Figure 3.3 presents the schematic wiring of the negative HV unit. During a MCE injection and separation, there is always at least one channel, which has to fulfill this task. This setup requires an additional HV unit, but it prevents the risk of debouncing or arc discharges. With this design, there is no theoretical upper limit for even higher voltages. To change the specifications of this instrument for adaptation to special applications, only the HV units, resistors and some software parameters have to be changed, but not the whole control and support structure.

3.3.2 Operation of the HVPS

The functionality of the HVPS was tested by monitoring the output voltages of all four channels. Figure 3.4 depicts the external measurement of all four channels during a voltage program similar to those used for real separations. An offset of about 100 V can be observed, which originates from the measurement equipment. Besides this, the demanded voltages can be provided in a reproducible way. The measurement frequency (250 Hz) is high enough to detect possible voltage oscillations or ramping effects, but these could not be observed in this case. The switching process can also be accurately monitored and the switching time is determined to be less than 50 ms from zero to 6 kV while connecting a buffer-filled chip.

Table 3.2: Voltage programs used for MCE separations. Injection time is 7 s.

| unit: V | | 2 kV | 4 kV | 6 kV |
|-----------|-----------|------------|------------|------------|
| reservoir | injection | separation | separation | separation |
| inlet | 1800 | 0 | 0 | 0 |
| waste | 3000 | 1000 | 1500 | 2000 |
| outlet | 0 | 2000 | 4000 | 6000 |
| sample | 1500 | 1000 | 1500 | 2000 |

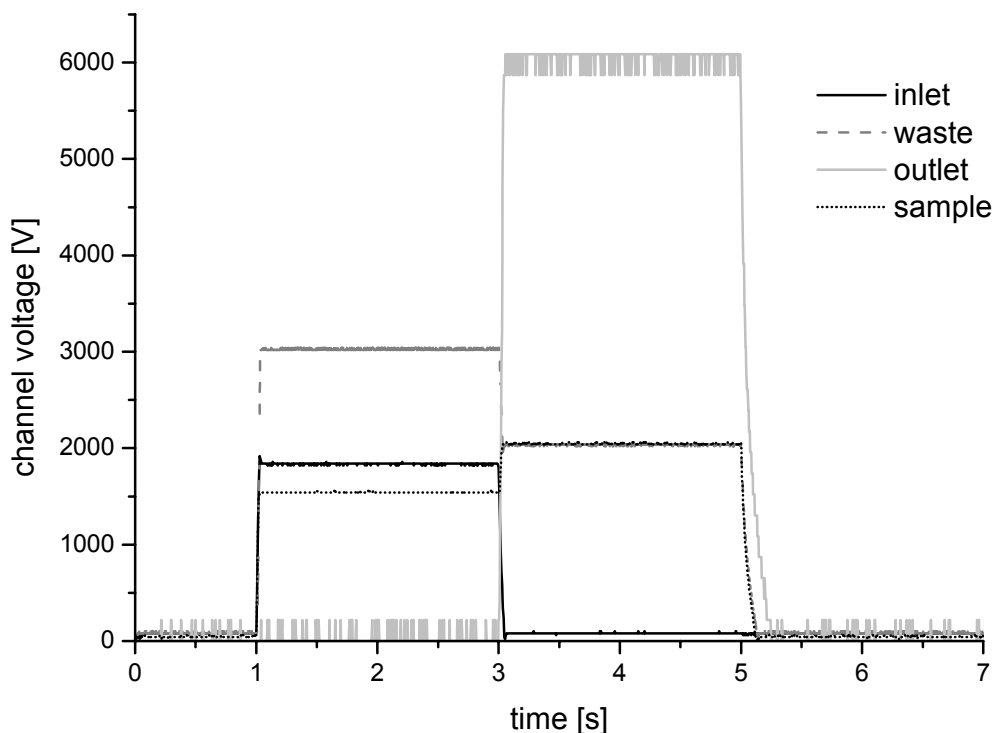


Figure 3.4: Measured switching and voltage of the HVPS connected to a buffer-filled microchip. 6 kV voltage program according to Table 3.2; step length 2 s. Measurement frequency at 250 Hz.

To visualize the necessity of a negative bias HV unit, the same program has been run without using this feature as depicted in Figure 3.5. Two effects can be observed. First, all channels set to zero, which are the outlet during injection and the inlet during the separation step, cannot deliver this potential and are shifted to elevated voltages. Second, when switching or at the end of the voltage program, it takes some time to reach the next voltage. Especially getting from 6 kV to a potential less state takes about one second.

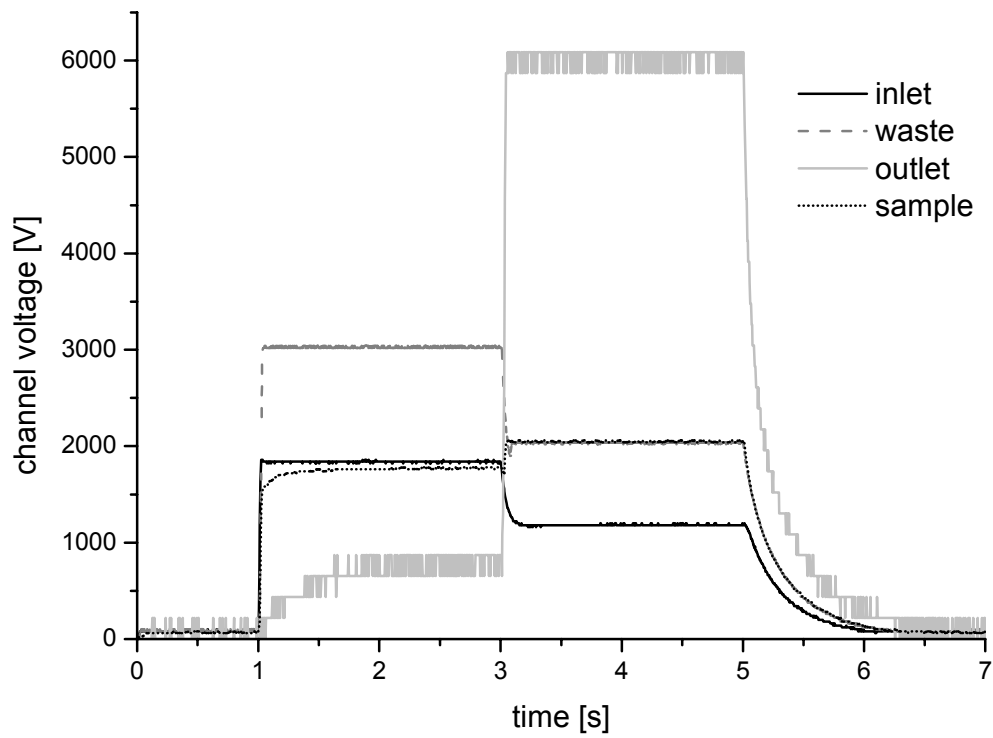


Figure 3.5: Measured switching and voltage of the HVPS while connected to a buffer-filled microchip and negative bias source switched off. 6 kV voltage program according to Table 3.2; step length 2 s.

3.3.3 Electrophoretic separations

The performance of the constructed instrument was tested on the separation of five SBD-thiol derivatives on a commercial glass microchip. A mixture of MAA, 2-MPA, 3-MPA, NA-Cys and GSH was derivatized with the fluorogenic reagent SBD-F. Figure 3.6 shows the electropherograms of three separations of this mixture with fluorescence detection in dependency of the separation voltage programs given in Table 3.2. During the separation step with 6 kV, the instrument measured a current of more than 400 μA at the output channel. This confirms the necessity of allowing currents in this range for successful separations.

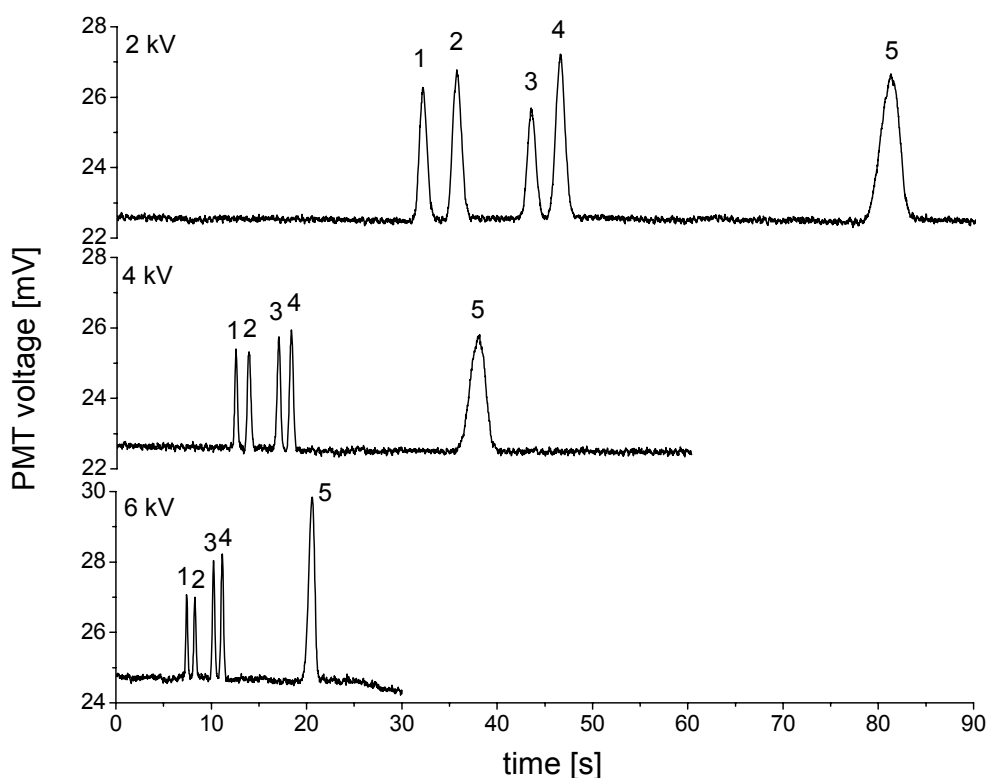


Figure 3.6: Comparison of the electropherograms of the separation of 5 SBD- thiol derivatives at 2, 4 and 6 kV separation voltages (see Table 3.2). Elution order: 1: MAA, 2: 2-MPA, 3: NA-Cys, 4: 3-MPA, 5:GSH.

Table 3.3 shows the calculated characteristics of the separations obtained with the three voltage programs. As expected, migration times of all compounds decrease with higher applied potentials. It is evident that peak areas decrease with higher applied voltages, as the analytes pass the detection volume faster due to their speed, which results in lower peak areas for non-destructive detectors. Although the calculated plates per separation are decreased with higher voltages, the peak width is significantly

decreased. Resolution of all peaks is not affected significantly, which is somehow surprising as the calculated plates of the separation are decreased. It can therefore be concluded that higher potentials offer the advantage of high separation speed (22 s at 6 kV versus 84 s at 2 kV) and improved peak shape (smaller and better to integrate).

Table 3.3: Peak characteristics of the separation of five SBD-thiol derivatives in dependency of the applied separation voltage. Presented values are the average of three experiments. SD: absolute standard deviations (n=3).

| voltage program | migration time [s] | SD | peak area [au] | SD | peak width [s] | SD | efficiency [plates] | SD | reso-lution [-] | SD |
|-----------------|--------------------|------|----------------|-------|----------------|------|---------------------|------|-----------------|------|
| MAA (1) | | | | | | | | | | |
| 2 kV | 32.54 | 0.61 | 3.312 | 0.223 | 0.94 | 0.02 | 6645 | 96 | - | - |
| 4 kV | 12.47 | 0.02 | 0.927 | 0.108 | 0.35 | 0.02 | 6990 | 798 | - | - |
| 6 kV | 7.39 | 0.06 | 0.708 | 0.133 | 0.24 | 0.01 | 5205 | 436 | - | - |
| 2-MPA (2) | | | | | | | | | | |
| 2 kV | 36.15 | 0.66 | 4.436 | 0.133 | 1.09 | 0.03 | 6107 | 276 | 1.39 | 0.06 |
| 4 kV | 13.81 | 0.05 | 1.17 | 0.162 | 0.42 | 0.01 | 5883 | 281 | 1.37 | 0.14 |
| 6 kV | 8.25 | 0.07 | 0.873 | 0.218 | 0.28 | 0.01 | 4799 | 331 | 1.19 | 0.14 |
| NA-Cys (3) | | | | | | | | | | |
| 2 kV | 44.21 | 0.89 | 3.122 | 0.105 | 1.02 | 0.03 | 10324 | 187 | 3.03 | 0.08 |
| 4 kV | 16.96 | 0.06 | 1.409 | 0.152 | 0.42 | 0.01 | 8871 | 517 | 2.93 | 0.27 |
| 6 kV | 10.23 | 0.11 | 1.190 | 0.218 | 0.29 | 0.00 | 6727 | 142 | 2.52 | 0.22 |
| 3-MPA (4) | | | | | | | | | | |
| 2 kV | 47.39 | 1.01 | 5.882 | 1.423 | 1.14 | 0.05 | 9560 | 420 | 1.20 | 0.03 |
| 4 kV | 18.27 | 0.05 | 1.642 | 0.204 | 0.47 | 0.00 | 8384 | 41 | 1.19 | 0.12 |
| 6 kV | 11.18 | 0.12 | 1.417 | 0.312 | 0.33 | 0.02 | 6295 | 673 | 1.16 | 0.07 |
| GSH (5) | | | | | | | | | | |
| 2 kV | 85.19 | 3.47 | 12.624 | 2.732 | 3.03 | 0.80 | 4910 | 2056 | 8.14 | 0.95 |
| 4 kV | 36.17 | 1.64 | 6.229 | 1.389 | 1.72 | 0.08 | 2446 | 145 | 7.30 | 0.98 |
| 6 kV | 21.60 | 1.28 | 5.147 | 1.564 | 0.72 | 0.10 | 5051 | 1083 | 6.94 | 0.83 |

3.4 Conclusions

This chapter describes the construction of a highly flexible four channel HVPS with an output voltage of 6 kV, 1 mA of current and voltage switching in less than 50 ms. This instrument is designed on a flexible technological platform without any high-voltage relays and therefore can be easily adapted by changing voltage modules fitting to the desired application like high-voltage or low priced. Four independent voltage sources enable the use of a large variety of chip designs and types of injection. The construction allows control by an external PC system via an USB port or alternatively by an additional small computing unit for non-laboratory use. Input data as well as measured voltage and current data are compatible with standard Microsoft Office software. To conclude, a robust all-purpose power supply for microchip capillary electrophoresis has been constructed and its use for highly efficient separations was demonstrated.

3.5 References

- [1] Janasek, D., Franzke, J., Manz, A., *Nature* **2006**, *442*, 374-380.
- [2] Revermann, T., Götz, S., Karst, U., **2007**, *submitted for publication*.
- [3] Harrison, D. J., Manz, A., Fan, Z. H., Ludi, H., Widmer, H. M., *Anal. Chem.* **1992**, *64*, 1926-1932.
- [4] Manz, A., Harrison, D. J., Verpoorte, E. M. J., Fettinger, J. C., Paulus, A., Ludi, H., Widmer, H. M., *J. Chromatogr.* **1992**, *593*, 253-258.
- [5] Dittrich, P. S., Tachikawa, K., Manz, A., *Anal. Chem.* **2006**, *78*, 3887-3907.
- [6] Collins, G. E., Wu, P., Lu, Q., Ramsey, J. D., Bromund, R. H., *Lab Chip* **2004**, *4*, 408-411.
- [7] Jacobson, S. C., Ermakov, S. V., Ramsey, J. M., *Anal. Chem.* **1999**, *71*, 3273-3276.
- [8] Erickson, D., Sinton, D., Li, D. Q., *Lab Chip* **2004**, *4*, 87-90.
- [9] Jackson, D. J., Naber, J. F., Roussel, T. J., Crain, M. M., Walsh, K. M., Keynton, R. S., Baldwin, R. P., *Anal. Chem.* **2003**, *75*, 3643-3649.
- [10] Renzi, R. F., Stamps, J., Horn, B. A., Ferko, S., VanderNoot, V. A., West, J. A. A., Crocker, R., Wiedenman, B., Yee, D., Fruetel, J. A., *Anal. Chem.* **2005**, *77*, 435-441.
- [11] Garcia, C. D., Liu, Y., Anderson, P., Henry, C. S., *Lab Chip* **2003**, *3*, 324-328.
- [12] Revermann, T., Götz, S., Karst, U., *Electrophoresis* **2007**, *accepted for publication*.

Chapter 4

Quantitative Analysis of Thiols in Consumer

Products on a Microfluidic Capillary

Electrophoresis Chip with Fluorescence Detection[‡]

A microchip capillary electrophoresis-based method for the quantification of the thiols mercaptoethanoic acid (MAA) and 2-mercaptopropionic acid (2-MPA) in depilatory cream and cold wave lotions was developed. The thiols were first derivatized with the fluorogenic reagent ammonium-7-fluorobenzo-2-oxa-1,3-diazole-4-sulfonate (SBD-F). The derivatives were separated within only 20 seconds by microchip capillary electrophoresis (MCE) and detected by their fluorescence. Conventional capillary electrophoresis with diode array detection and liquid chromatography with fluorescence detection were used for validation. The internal standard 3-mercaptopropionic acid (3-MPA) provided relative standard deviations of multiple injections of only 4 % or less for the MCE approach. Limit of detection is 2 μM , limit of quantification 6 μM and the linear range comprises nearly three decades of concentration starting at the limit of quantification.

[‡]Revermann T, Götz S, Karst U, **2007**, accepted for publication (Electrophoresis)

4.1 Introduction

In the last few years, intense research activities were directed towards the miniaturization of analytical methods, with a particular focus on the design and use of microchips [1, 2]. Although many attractive approaches have been published, most of them were presented as proof of principle only. Few papers, however, focus on the truly quantitative analysis on microchips. Capillary electrophoresis is one of the driving forces used in microchip technology due to its separation efficiency for polar analytes.

The determination of inorganic ions, e.g. lithium in blood [3, 4], anions and cations in tap water [5], nitrite in water [6] and calcium in urine [7], has been described. While most of this work relies on capillary zone electrophoresis (CZE), isotachophoretic approaches have been described as well [8, 9]. Further examples for quantitative MCE include organic molecules like oxalate in urine [10], carnitines in water [11], 4-amino-3-methyl-N-ethyl-N-(β -methane sulfonamidoethyl)aniline in photographic developer [12], levoglucosan in aerosols [13], thiols in nerve agent degradation products [14] and homocysteine in plasma [15]. Semi-quantitative approaches are known for biological and medical applications like DNA in restriction digests of adenovirus 2 [16] and hepatitis C viruses in clinical patients [17].

Different detection principles can be combined with CE or MCE such as optical methods, electrochemical detection or even mass spectrometry [18-21]. Optical techniques are well established and have the advantage of freely selecting the detection volume on an existing glass microchip. Fluorescence detection is generally more sensitive than UV detection and frequently, derivatization reactions have to be carried out. The derivatization of thiols has two major reasons: One is to stabilize the reactive thiol functionality, because thiols are known to form sulfide bridges and can easily be oxidized [22]. The second is an increase in the sensitivity of detection. Many different labeling agents are known for the derivatization of thiols [22, 23]. 7-Fluorobenzo-2-oxa-1,3-diazole-4-sulfonate (SBD-F, Figure 4.1) has an incorporated negative charge in the sulfonyl functionality. It is highly water-soluble and easily amenable to electrophoresis. Furthermore, it is highly reactive towards thiol groups and, in contrast to the reaction products, the reagent itself is not fluorescent [24]. It is also known for its excellent stability, as it is stable in borate buffer (pH 9.5) at room temperature for at least one week [25]. Dissolved SBD-thiol derivatives can be stored for more than a week in the refrigerator. Fluorescence is measured with excitation at 380 nm and emission at 515 nm for most SBD thiol derivatives [24].

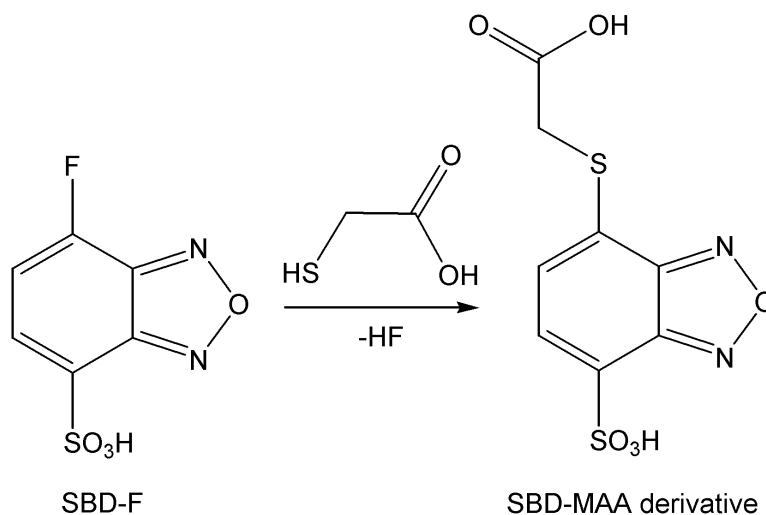


Figure 4.1: Structure of the SBD-F reagent and its reaction with MAA.

Commercial depilatory cream and cold wave lotions contain mercaptoethanoic acid (MAA) (also known as mercaptoacetic acid or thioglycolic acid), 2-mercaptopropionic acid (2-MPA) (thiolactic acid) or a mixture of these [26]. According to German legislation, depilatory cream for private use may contain up to 5% and cold wave lotions may contain up to 8% of this acid (11 % for professional use) [27]. These concentrations are calculated as of the free acid. The standard procedure for the determination of the thiol content proposed by EU legislation is an iodometric titration. As titrations do always yield a sum parameter, a GC analysis after derivatization is suggested for samples containing more than one thiol. This GC analysis employs overnight derivatization with diazomethane as derivatization agent after precipitation of thiols with cadmium acetate [28].

In this chapter, the development of a new method for the determination of thiols in cosmetics after their derivatization with SBD-F is reported. A CE-DAD method is developed and transferred to MCE-Fluorescence and compared to the results of HPLC-Fluorescence measurements. Microchip analysis requires only small amounts of sample and reagent and separation times can be reduced compared to conventional methods.

4.2 Materials and methods

4.2.1 Materials, chemicals and samples

Boric acid, EDTA, sodium hydroxide and citric acid were purchased from Merck (Darmstadt, Germany). Mercaptoethanoic acid (MAA), 2-mercaptopropionic acid (2-MPA) and 3-mercaptopropionic acid (3-MPA) were obtained from Aldrich (Steinheim, Germany). Hydrochloric acid was purchased from Acros (Geel, Belgium) and water was purified by a Millipore-Q plus water cleaning system from Millipore (Billerica, MA, USA). SBD-F was synthesized according to literature [24, 29].

Ten cold wave lotions and depilatory cream samples from different manufacturers were purchased from retail stores in Germany, The Netherlands and the United States. Two samples were cold wave lotions; eight were different types of depilatory creams like cream, mousse or foam.

4.2.2 Buffer and standard preparation

The 50 mM borate buffer pH 9.50 containing 5 mM of EDTA was prepared by weighing in solid substances. After adding 800 mL of Milli-Q water, it was titrated with 1 M or 100 mM sodium hydroxide solution to a pH of 9.5 prior to filling up to 1 L. Citrate running buffers were prepared in the same way, and stored at 4°C. All buffers were filtered through a 0.45 µm nylon syringe filter (Alltech, Breda, The Netherlands) after preparation.

Thiol standards were prepared by dissolving the thiols in borate buffer. For all further dilutions and mixings, borate buffer was used as aqueous solvent. A 30 to 40 mM solution of 3-MPA was made to add this compound as internal standard before derivatization.

4.2.3 Derivatization procedure and sample preparation

Between one and two milligrams of cream sample were suspended in 0.5 ml of borate buffer. Then, the internal standard (3-MPA) solution and 470 µl less the volume of the previously added internal standard solution, of a 10 mM SBD-F solution in reaction buffer were added. It is useful to subtract the volume of the internal standard solution from the reagent, as then the

analysis is always performed with the same volume, even if on another day a differently concentrated 3-MPA solution is used. The closed vial was heated in a water bath at 60°C for one hour. After cooling down to room temperature, 30 µl of 2 M hydrochloric acid were added to acidify the solution. These minor modifications were applied compared to the suggested reaction parameters described in reference [30] to adjust the analysis procedure to the requirements of MCE.

For cold wave lotions and thiol standards, the same basic derivatization procedure was followed, but for these, the diluted sample (with borate buffer) or calibration standards prepared in borate buffer were used. All measurements were performed within one week after derivatization and storage of the solutions at 4°C, which is, according to reference [30], a reasonable timescale for storage of dissolved SBD-derivatives.

4.2.4 CE, MCE and HPLC separation conditions

CE experiments were performed on an Agilent HP^{3D}CE instrument equipped with a diode-array detector (Agilent, Waldbronn, Germany). Fused silica capillaries with an outer diameter of 363 µm were obtained from Polymicro Technologies (Phoenix, AZ, USA). CE separations were performed on a 32 cm long capillary with an effective length of 23.5 cm and an inner diameter of

75 μm . Prior to each series of experiments, capillaries were conditioned for 25 min with 1 M NaOH solution and were then flushed with water and citrate running buffer (one minute each). The running buffer had a pH of 4.36 with an ionic strength of 20 mM. Between the measurements, the capillary was flushed for half a minute with buffer from a separate vial into a waste vial. Samples were introduced hydrodynamically by applying a pressure of 50 hPa for 1 s. A separation voltage of -28 kV was applied for 1.3 min. To detect SBD-thiol derivatives, an absorption wavelength of 383 nm was selected and 320 nm were used for detecting the SBD-F reagent.

T3550 glass microchips for capillary electrophoresis were purchased from Micronit Microfluidics (Enschede, The Netherlands) with a channel width of 50 μm and depth of 20 μm . A channel of 5 mm length transports buffer or sample solutions to the injector. The separation path length is 35 mm with 26 mm from the double tee injector to the position of the detection volume. An ECH-135L high voltage power supply (Micronit Microfluidics) with a custom made outlet for a TTL trigger signal was combined with an in-house built chip holder including platinum electrodes made from Pt wire (0.25 mm diameter). Samples were introduced by a pinched injection and separated using the voltage program given in Table 4.1. Microchip separations were performed with a 100 mM citrate buffer pH 4.36. The chip was flushed with buffer and all reservoirs were refilled with 2.5 μl solution prior to each measurement. Flushing of microchip channels was performed with a 500 μl

syringe (SGE, Ringwood, Australia) equipped with a Teflon liner (Upchurch Scientific, Oak Harbor, WA, USA). Voltages were applied according to Table 4.1.

Table 4.1: Voltages applied to the microchip reservoirs.

| Reservoir | injection (10 s) [V] | separation (30 s) [V] |
|--------------|----------------------|-----------------------|
| Sample | 1500 | 1000 |
| sample waste | 3000 | 1000 |
| Buffer | 1800 | 0 |
| Buffer waste | 0 | 3000 |

HPLC measurements were performed using a Shimadzu (Duisburg, Germany) HPLC system consisting of two LC-10AS pumps, GT-154 degasser unit, SIL-10A autosampler, SPD-M10Avp diode array detector, RF-10AXL fluorescence detector, and CBM-10A controller unit with class LC-10 software version 1.6. A 4.6 x 150 mm Eclipse C8 RP column (Agilent, Waldbronn, Germany) with 5 μ m particles was used for LC separations. The mobile phase consisted of acetonitrile (ACN) and 20 mM phosphate buffer at pH 3.0 and was used for gradient elution. In the first four minutes, the ACN content was changed from 10 to 20 %. In the following three minutes, it was gradually increased up to 40%.

4.2.5 Fluorescence microscope and data analysis

The fluorescence microscope-based setup consists of an inverse IX-71S1F fluorescence microscope (Olympus, Hamburg, Germany), an Olympus xenon burner (U-LH75XEAP0), a SpectraPro 308i spectrograph (Acton Research, Acton, MA, USA) equipped with a 150 grooves per mm (gr/mm) grating and a light intensified CCD-camera PI-Max 512RB from Princeton Instruments (Trenton, NJ, USA) was combined with a ST133 controller ver.5 (Princeton Instruments). Data recording and evaluation was performed by WinSpec/32 software version 2.5.12.0 (Princeton Instruments). For wavelength selection, a filter cube with components from Chroma (Rockingham, VT, USA) was employed (exciter: D390/70X 104733; dichroic: 440DCXR; emitter: HQ500LP 47767). This setup can be used in combination with the commercial CE instrument or for detection of microchip separations. For a detailed description of this detector see reference [31]. After exporting the raw data, all electropherograms were integrated using HP ^{3D}CE ChemStation software revision A 08.03 (Agilent, Waldbronn, Germany).

Fluorescence spectra were recorded by an Aminco Bowman series 2 fluorescence spectrophotometer (now Thermo Electron, Dreieich, Germany) with AB 2 software version 5.00. Measurements with organic solvents contain 10% of aqueous borate buffer at pH 9.5.

4.3 Results

4.3.1 Fluorescence properties of SBD-thiol derivatives

In order to determine the properties of the SBD-thiol derivatives for CE separation and detection, the effects of buffer composition and pH on fluorescence intensities and emission wavelength were tested. It is well known, that the fluorescent properties SBD-thiol derivatives are sensitive to solvent and pH value [30]. In Figure 4.2 fluorescence spectra of four different thiol-SBD derivatives are presented. Excited at 380 nm, the wavelength of the intensity maxima varies slightly depending on the individual thiol. The emission maximum of the acetyl cysteine derivative (528 nm), for example, is 7 nm lower than that of 2-MPA (535 nm) under the given conditions.

In contrast to the SBD-cysteine derivative [30], the mercaptoethanoic acid derivative does not show a significant pH dependence on its fluorescence intensity. However, fluorescence intensities can well be altered by addition of organic solvents (Figure 4.3).

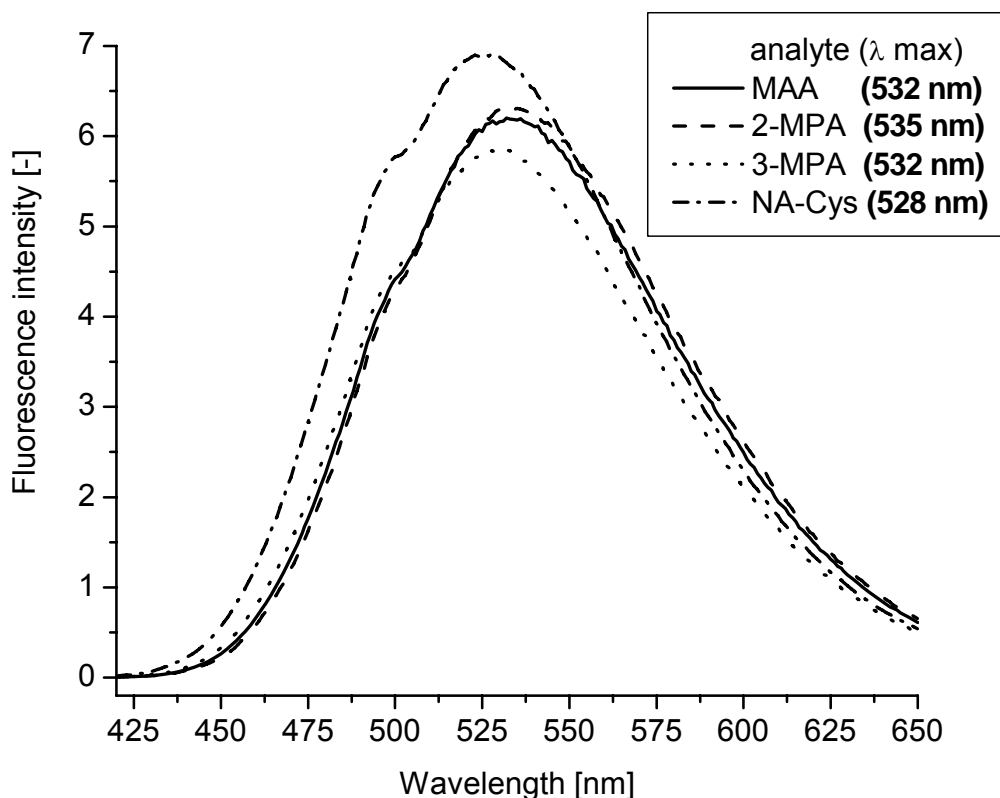


Figure 4.2: Fluorescence emission spectra of four different thiol-SBD derivatives recorded with an excitation wavelength of 380 nm in aqueous borate buffer pH 9.5 containing 5 mM EDTA.

The highest intensities were obtained by the addition of ethanol or ethylene glycol with an increase of a factor of approximately four compared with an aqueous solution at pH 9.5, which is sodium borate buffered. Slightly higher intensities than with this borate buffer were obtained after addition of methanol, acetone, DMSO and ACN. Lower intensities were obtained after the addition of ethyl acetate. Dissolving the derivatives in organic solvents results in a shift of emission maxima to lower wavelengths.

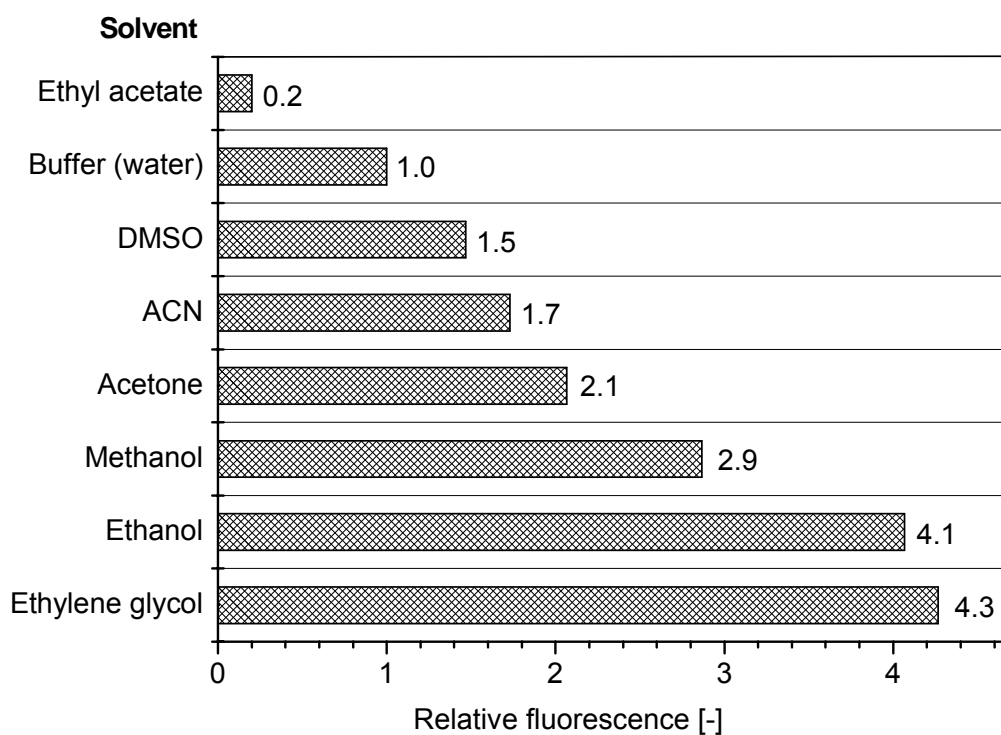


Figure 4.3: Relative fluorescence intensities of the MAA-SBD derivative in different organic solvents (containing 10 % aqueous reaction solution).

The addition of a solvent with an alcohol moiety (ethanol, methanol and ethylene glycol) lowers the wavelength by approximately 15 nm; for all other tested organic solvents, a shift of approximately 35 nm was observed.

4.3.2 Optimization of electrophoretic separations

The non-derivatized thiols as well as the internal standard are weak acids. After derivatization, the acid functionality remains unaltered and the SBD-F reagent adds a sulfonyl functionality. Therefore all molecules are negatively charged, which renders the derivatives to be quickly moving in the negative CE mode.

Different pH values and compositions were tested in this work. Fine-tuning of the pH value in the range of pH 3.79 to pH 4.50 of a sodium citrate buffer is shown in Figure 4.4. By changing the pH value of the running buffer from 3.79 to 4.27, the elution order is changed and the SBD-F peak is shifted to the end of the separation. The separation is completed after 48 s using a pH of 4.50 compared to 70 s (pH 3.79). Peak shape is also changing during this series. Running buffer of pH 4.36 yielded the most symmetric peaks. A 20 mM sodium citrate buffer with a pH value of 4.36 was finally selected due to the parameters elution order, separation time and peak shape. Generally, it is advantageous to have the reagent peak eluting last, as there are no interferences with analyte peaks to be expected and as the measurement may be stopped earlier. This requirement is well achieved in the described separation system.

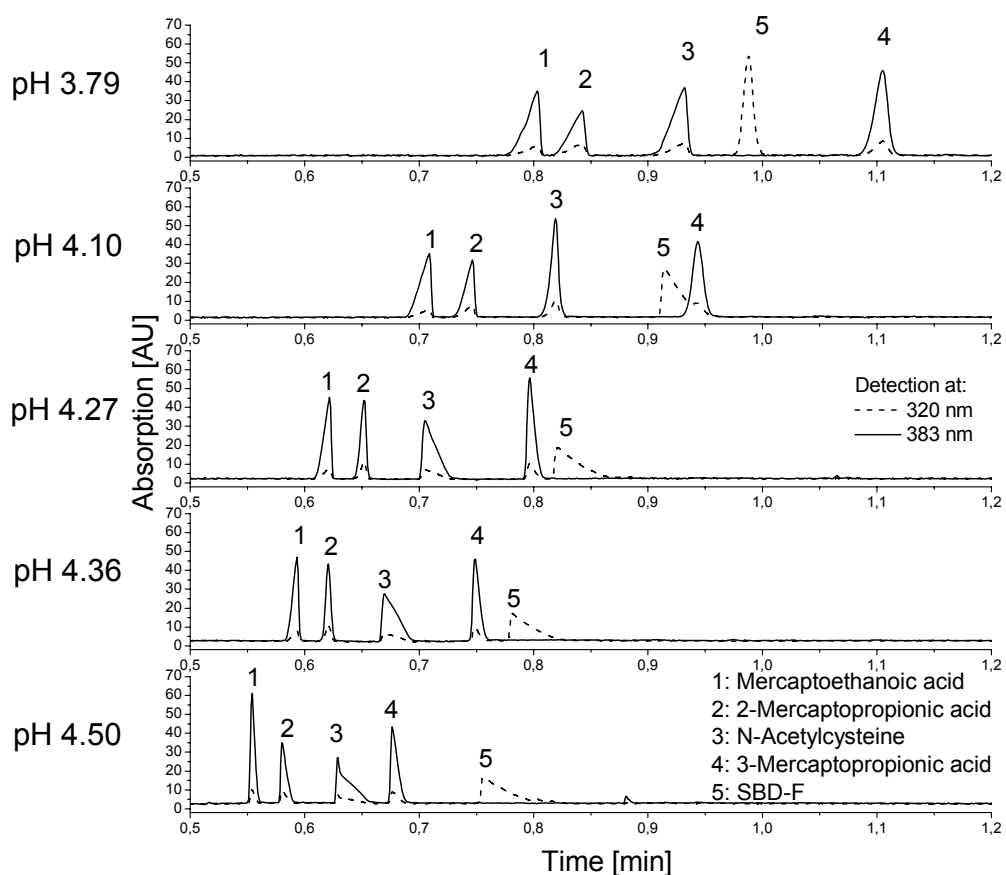


Figure 4.4: Optimization of the pH value of the separation buffer. A reaction mixture of four different thiol-SBD derivatives was used to test the separation conditions. A solution containing each thiol in 1 mM concentration before derivatization was employed. Electropherograms were recorded on a CE-DAD system.

4.3.3 Microchip separations

Figure 4.5 depicts an Electropherogram of the separation of a solution containing three different SBD-thiol derivatives (MAA, 2-MPA, 3-MPA). This separation was obtained after transferring the method from the CE-DAD system to the microchip. As fluorescence is used for detection on the microchip, the SBD-F reagent is not detected, but it is expected to elute after the last peak as the peak order is the same compared to conventional CE. A 100 mM concentration of the running buffer was selected for this technique, as injections worked better due to the similarity of electrolyte concentration in sample solutions and running buffer.

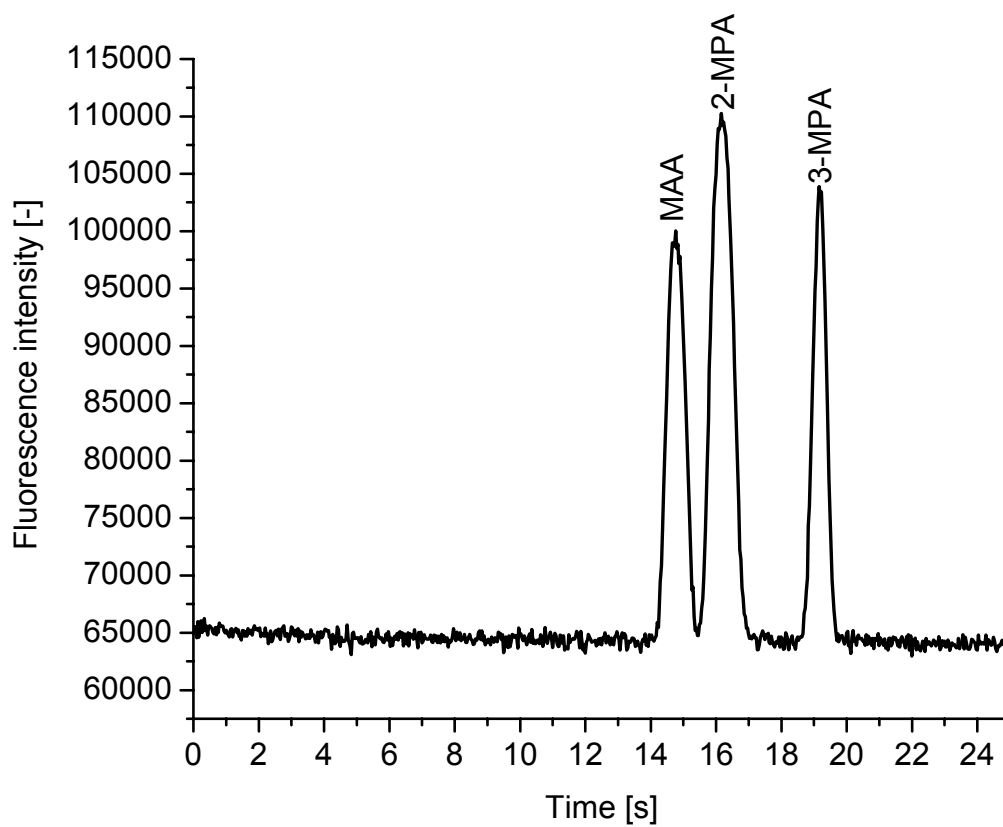


Figure 4.5: Electropherogram of a mixture of three different thiols (1 mM MAA, 2 mM 2-MPA and 10 mM 3-MPA) obtained from a microchip separation with fluorescence detection.

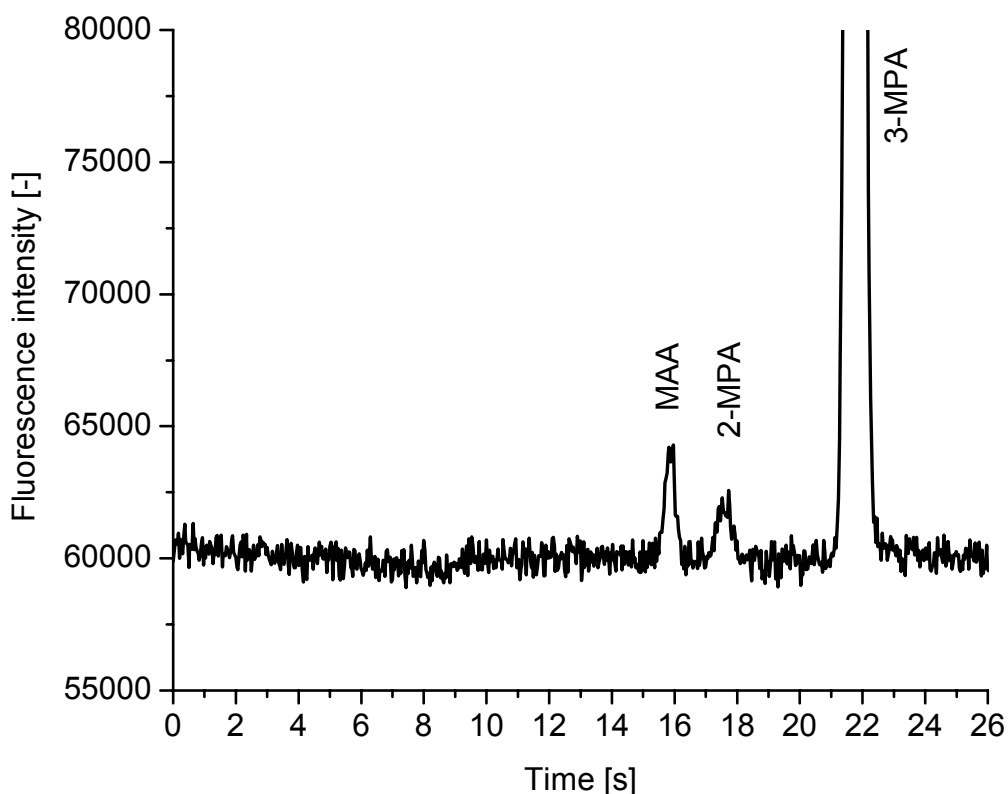


Figure 4.6: Microchip electropherogram of a calibration standard at LOD (0.002 mM MAA, 0.002 mM 2-MPA and 1 mM 3-MPA).

For determination with MCE, an internal standard is essential to correct for experimental errors. Figure 4.6 shows an electropherogram of MAA and 2-MPA derivatives obtained at LOD conditions with the 3-MPA derivative added as internal standard. A separation of a derivatized cold wave lotion, spiked with 3-MPA is presented in Figure 4.7. The biggest source of error is related to the coupling of the microchip with the detector. Although the microchip is fixed by the chip holder, there is still some variability, so that the separation channel is not necessarily projected into the entrance slit of the

spectrograph. Using a 40 fold magnification objective instead of 20 fold magnification reduces the experimental error to less than 10% RSD. After employing an internal standard, the variations of the peak area were reduced to a level comparable with conventional CE measurements (less than 4 % RSD). This procedure also corrects for various other experimental errors made during measurement (injection, unstable detection / excitation) or errors done in sample preparation.

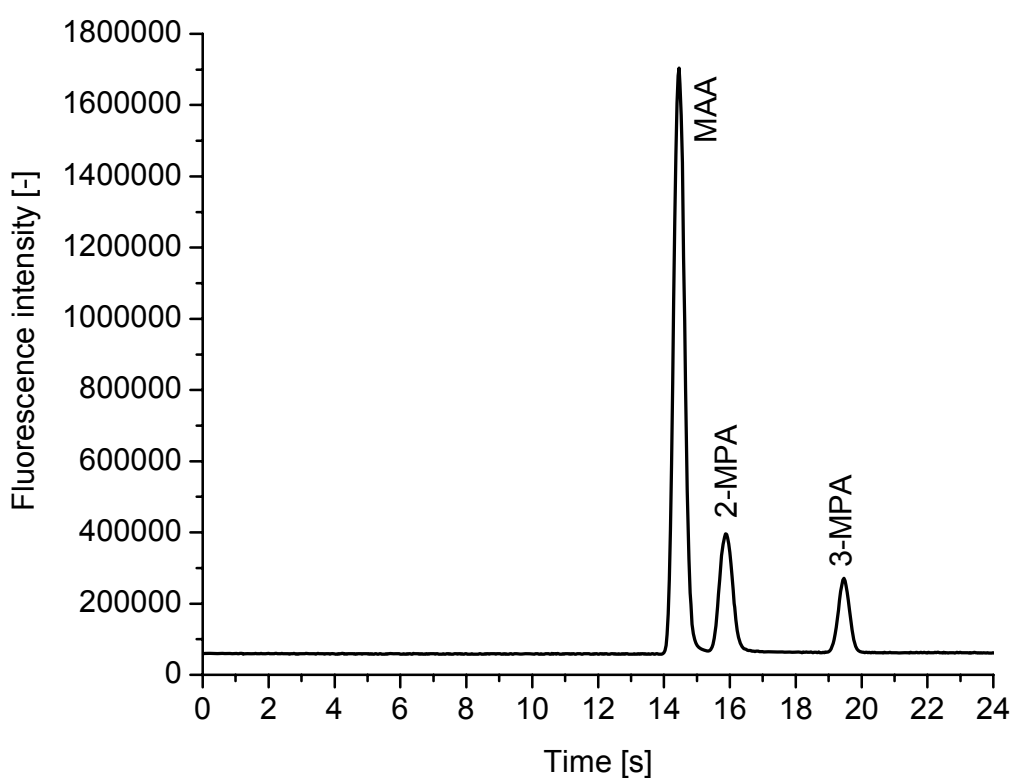


Figure 4.7: Electropherogram of a cold wave lotion (595 μg “Welle strong” in 1 ml reaction solution containing 1 mM 3-MPA as internal standard) obtained from MCE-fluorescence.

4.3.4 Comparison of HPLC, CE and MCE measurements

On-chip measurements were compared with results obtained from CE-DAD and HPLC-Fluorescence instruments. All three instruments were therefore tested with the same set of solutions. All stated concentrations are concentrations of thiol before derivatization and dilutions were also made before derivatizing the solutions. Limits of detection for MAA were 20 μM for the CE-DAD system. A LOD of 2 μM was determined for on-chip measurements with fluorescence detection. The LOD value for HPLC-Fluorescence is also 20 μM . Solutions for HPLC measurements were diluted by a factor of 100, as the undiluted, highest concentrated solution provides a signal exceeding the upper limit of the fluorescence detector. This means that the detection limit of the instrument is theoretically one decade lower than achieved by MCE if the undiluted samples would be used.

The linear range for the determination of thiols is 50 μM to 2 mM for CE-DAD and HPLC-Fluorescence and 5 μM to 2 mM for MCE-Fluorescence measurements. At the lower end, the range is restricted by the quantification limit of the analytical instrumentation and the upper end is limited by the excess of reagent. A detailed description of the comparison of analytical results for the quantification is presented in the following paragraph.

4.3.5 Quantification of thiols in depilatory cream and cold wave lotions

Thiol concentrations in ten different cosmetic samples were determined by three different instruments: CE-DAD, HPLC-Fluorescence and MCE-Fluorescence. Calibration parameters for all three instruments are given in Table 4.2. Table 4.3 shows the mass percentage of thiol in different depilatory creams and cold wave lotions. After applying all described corrections, RSD values for three repeated measurements are below 4 % ($n = 3$) and the determined values of thiol content of MCE and HPLC are within the error margins. CE-DAD measurements tend to give a lower result. The application of the internal standard does not only decrease the RSD values of the microchip measurements, but it is also the base for the validation of the data by HPLC and conventional CE.

Table 4.2: Calibration parameters for MCE, CE-DAD and HPLC measurements.

Constants A and B are the parameters for the line equations of the type

$$Y = A + B \cdot X.$$

| | | A | B | n | R ² |
|------|-------|---------|---------|---|----------------|
| MCE | MAA | 3568 | 801838 | 5 | 0.9999 |
| | 2-MPA | 3496 | 489804 | 5 | 0.9995 |
| HPLC | MAA | -2264 | 142353 | 5 | 0.9999 |
| | 2-MPA | 1789 | 80653 | 5 | 0.9997 |
| CE | MAA | 0.35559 | 9.42952 | 5 | 0.9999 |
| | 2-MPA | 0.32221 | 9.08173 | 5 | 0.9986 |

Table 4.3: Determined MAA and MPA contents of 9 depilatory creams and 2 cold wave lotions in mass percent; results for all three detection systems are shown with their corresponding standard deviations (n = 3).

| Mass % MAA | MCE | % RSD | HPLC | % RSD | CE | % RSD |
|----------------------|------|-------|------|-------|------|-------|
| depilatory creams | | | | | | |
| Isana | 2.37 | 2.91 | 2.48 | 1.82 | 2.10 | 2.80 |
| Nair | 3.30 | 0.27 | 3.30 | 1.49 | 2.88 | 2.01 |
| Sally Hansen | 2.96 | 0.80 | 3.02 | 0.81 | 2.70 | 1.63 |
| Veet "rosa" | 4.44 | 0.61 | 4.48 | 0.77 | 3.84 | 2.20 |
| Veet "blau" | 3.22 | 1.73 | 3.30 | 0.95 | 2.75 | 4.00 |
| Pilca (creme) | 2.77 | 2.06 | 2.96 | 0.81 | 2.41 | 2.74 |
| Pilca (mousse) | 4.00 | 1.22 | 4.36 | 1.68 | 3.47 | 1.85 |
| Snä | 6.11 | 3.88 | 6.42 | 1.70 | 5.01 | 1.81 |
| Cold wave lotions | | | | | | |
| "mild" | 7.00 | 3.43 | 7.72 | 0.05 | 5.69 | 3.47 |
| "strong" MAA | 6.85 | 2.51 | 7.47 | 0.92 | 5.57 | 0.63 |
| "strong" MPA | 3.01 | 1.83 | 3.05 | 1.64 | 2.10 | 0.83 |

4.4 Conclusions

A new analytical method for the quantification of thiols in depilatory cream and cold wave lotions was developed. The developed separation conditions for the commercial CE system were transferred to the MCE format. On the chip, a baseline separation including an internal standard was achieved in 20 seconds. It was demonstrated that the results obtained by microchip capillary electrophoresis are comparable to those achieved by using established instruments like HPLC. Quantitative results of MCE are in good agreement with HPLC measurements and RSD values are below 4% for MCE separations after correction by an internal standard. For analysis, only small amounts of sample and reagents are necessary and glass microchips could easily be reused multiple times.

Future work will deal with the integration of the derivatization on chip and automation of microchip rinsing and filling procedures in order to further improve robustness and reproducibility of the microchip technology.

4.5 References

- [1] Reyes, D. R., Iossifidis, D., Auroux, P. A., Manz, A., *Anal. Chem.* **2002**, *74*, 2623-2636.
- [2] Auroux, P. A., Iossifidis, D., Reyes, D. R., Manz, A., *Anal. Chem.* **2002**, *74*, 2637-2652.
- [3] Vrouwe, E. X., Luttge, R., van den Berg, A., *Electrophoresis* **2004**, *25*, 1660-1667.
- [4] Vrouwe, E. X., Luttge, R., Olthuis, W., van den Berg, A., *Electrophoresis* **2005**, *26*, 3032-3042.
- [5] Vrouwe, E. X., Luttge, R., Olthuis, W., van den Berg, A., *J. Chromatogr. A* **2006**, *1102*, 287-293.
- [6] Greenway, G. M., Haswell, S. J., Petsul, P. H., *Anal. Chim. Acta* **1999**, *387*, 1-10.
- [7] Malcik, N., Ferrance, J. P., Landers, J. P., Caglar, P., *Sens. Actuator B-Chem.* **2005**, *107*, 24-31.
- [8] Masar, M., Zuborova, M., Bielcikova, J., Kaniansky, D., Johnck, M., Stanislawski, B., *J. Chromatogr. A* **2001**, *916*, 101-111.
- [9] Bodor, R., Madajova, V., Kaniansky, D., Masar, M., Johnck, M., Stanislawski, B., *J. Chromatogr. A* **2001**, *916*, 155-165.
- [10] Zuborova, M., Masar, M., Kaniansky, D., Johnck, M., Stanislawski, B., *Electrophoresis* **2002**, *23*, 774-781.

- [11] Kameoka, J., Craighead, H. G., Zhang, H. W., Henion, J., *Anal. Chem.* **2001**, 73, 1935-1941.
- [12] Sirichai, S., de Mello, A. J., *Analyst* **1999**, 125, 133-137.
- [13] Garcia, C. D., Engling, G., Herckes, P., Collett, J. L., Henry, C. S., *Environ. Sci. Technol.* **2005**, 39, 618-623.
- [14] Wang, J., Zima, J., Lawrence, N. S., Chatrathi, M. P., Mulchandani, A., Collins, G. E., *Anal. Chem.* **2004**, 76, 4721-4726.
- [15] Pasas, S. A., Lacher, N. A., Davies, M. I., Lunte, S. M., *Electrophoresis* **2002**, 23, 759-766.
- [16] Mueller, O., Hahnenberger, K., Dittmann, M., Yee, H., Dubrow, R., Nagle, R., Ilsley, D., *Electrophoresis* **2000**, 21, 128-134.
- [17] Young, K. C., Lien, H. M., Lin, C. C., Chang, T. T., Lee, G. B., Chen, S. H., *Talanta* **2002**, 56, 323-330.
- [18] Uchiyama, K., Nakajima, H., Hobo, T., *Anal. Bioanal. Chem.* **2004**, 379, 375-382.
- [19] Schwarz, M. A., Hauser, P. C., *Lab Chip* **2001**, 1, 1-6.
- [20] Mogensen, K. B., Klank, H., Kutter, J. P., *Electrophoresis* **2004**, 25, 3498-3512.
- [21] Vandaveer, W. R., Pasas-Farmer, S. A., Fischer, D. J., Frankenfeld, C. N., Lunte, S. M., *Electrophoresis* **2004**, 25, 3528-3549.
- [22] Shimada, K., Mitamura, K., *J. Chromatogr. B-Biomed. Appl.* **1994**, 659, 227-241.

- [23] Waterval, J. C. M., Lingeman, H., Bult, A., Underberg, W. J. M., *Electrophoresis* **2000**, *21*, 4029-4045.
- [24] Imai, K., Toyo'oka, T., *Anal. Biochem.* **1983**, *128*, 471-473.
- [25] Imai, K., Uzu, S., Toyooka, T., *J. Pharm. Biomed. Anal.* **1989**, *7*, 1395-1403.
- [26] Falbe, J., Regitz, M., *Römpf Lexikon Chemie*, Georg Thieme Verlag, Stuttgart, **1999**, pp. 2594, 4523, 4525-4526.
- [27] Horst, M., Mrohs, A., *Lebensmittelrecht auf CD-Rom*, Behr's Verlag GmbH & Co. KG, Hamburg **2005**, Kosmetik-Verordnung vom 7. Oktober 1997.
- [28] European Commission, E. D.-G., Pharmaceuticals and cosmetics: Cosmetics legislation, Cosmetic Products, Vol. 2: Methods of analysis, Office for Official Publications of the European Communities, Luxembourg, **2000**, pp. 80-88.
- [29] Di Nunno, L., Florio, S., Todesco, P. E., *J. Chem. Soc. (C)* **1970**, 1433-1434.
- [30] Toyo'oka, T., Imai, K., *Analyst* **1984**, *109*, 1003-1007.
- [31] Götz, S., Karst, U., *Sens. Actuator B-Chem.* **2007**, *in press*, DOI:10.1016/j.snb.2006.1008.1027.

Chapter 5

Quantitative On-Chip Determination of Taurine in Energy and Sports Drinks[‡]

A new method for the quantitative determination of taurine in beverages by microchip electrophoresis was developed. A rapid and simple sample preparation procedure, only including two dilution steps and the addition of the fluorogenic labeling reagent NBD-Cl (4-chloro-7-nitrobenzofurazan), is applied. Using a home-built wavelength-resolved fluorescence detector, the separation and determination of the taurine derivative could be achieved in only 12 seconds, while the additional spectral information was utilized to ensure peak purity. Spanning from 0.1 to 50 mmol/L, the linear dynamic range of the applied method was adapted to the apparent contents in common taurine containing beverages. The smallest detectable amount of the taurine derivative actually injected into the separation channel was as low as 60 amol. The method was successfully validated by an independent liquid chromatographic method.

[‡]Götz S, Revermann T, Karst U, *Lab chip* **2007**, 7, 93-97

5.1 Introduction

Since first appearances of lab-on-a-chip applications [1] and the proposal of micro total analysis systems [2], many researchers were fascinated by the apparent advantages of miniaturized separation and detection systems. Ultra short separation times on low-cost disposable devices combined with a strongly reduced amount of sample and organic solvents needed encouraged a large number of research groups to work in this field. Because of the fact that no pumps or pressure-tight connections to the macro world were needed, electrophoretic separations could most easily be adapted to the dimensions of microchips [3] and are still mainly used today. Combined with fluorescence detection, electrophoresis offers very favorable selectivity and sensitivity, rapid separations and very high separation efficiencies. In the following years, many impressive results have been reported, ranging from ultra-trace detection [4] and on-chip derivatization [5] to single cell lysis experiments [6] and ultra fast chiral separations [7]. Despite all the advances made in this area, most of the remarkable work published is of qualitative or semi-quantitative nature. On-chip electrophoresis still suffers from bad reproducibility compared to the results of desktop instruments; analytical figures of merit are often extrapolated or calculated from signal-to-noise ratios of single measurements. Only few reports of truly quantitative on-chip determinations with real samples can be found in literature. Inorganic ions, such as nitrite in water [8], calcium in urine [9] and lithium in blood [10] as well as a few more complex analytes e.g. levoglucosan in aerosols [11],

thiols in nerve agent degradation products [12] and homocysteine in plasma [13] have been determined. Many problems associated with miniaturized separation and detection systems, like pH-changes due to electrolysis [14-16], analyte surface interactions [17] and temperature effects [18], have already been addressed and often solved, but mostly in a way not suited for routine use.

Taurine (2-aminoethansulfonic acid) is a semi-essential amino acid, which is abundant in high concentrations in many tissues and body fluids. Although it is not incorporated into proteins, taurine in its free form is associated with a vast variety of physiological functions, such as antioxidation activity [19], neuromodulation, membrane stabilization [20] and modulation of intracellular calcium levels [21]. While in a healthy state, intercellular taurine levels are strictly controlled, altered concentrations in plasma and urine have been associated with a variety of diseases including epilepsy [22], myocardial infarction [23] and cancer [24]. With regard to the importance of taurine in retinal development, reproduction and development, it has been added to infant formula as well as to parental solutions [25]. In recent years, with the propagation of energy and sports drinks, the normal daily uptake of taurine could easily be exceeded by a factor of 100. Although animal studies have not indicated toxic effects of taurine, the need for a rapid and easy method of taurine determination in food and beverages for quality assurance and product control purposes has become more important.

While taurine can be detected directly by means of pulsed amperometric detection [26], the most frequently used method for taurine determination is the HPLC separation with subsequent UV/vis or fluorescence detection [27]. The required derivatization reagents include *o*-phthalaldehyde [28], 2,4-dinitrofluorbenzene [29] and fluorescamine [30,31]. In recent years, alternative separation methods like ion-exchange chromatography [32] and particularly capillary electrophoresis [33] became more prominent.

In this chapter, the quantitative determination of taurine in sports drinks and other taurine containing beverages by means of a very rapid on-chip CE separation and wavelength-resolved fluorescence detection is presented. The applied detector system consisting of a fluorescence microscope, a spectrograph and an intensified CCD-camera delivers information-rich 3-dimensional electropherograms comparable to diode-array detection in UV/vis spectroscopy. This set-up is the first wavelength-resolved detection system specially adapted to the requirements of rapid on-chip separations. More fundamental information about wavelength-resolved detection systems for non-microchip CE applications can be found in the comprehensive review by Sweedler et al [34]. This chapter describes a fast and easy way of receiving reliable data with reproducibility comparable to other established methods.

5.2 Experimental

Taurine standard solutions were derived by dilution from a freshly prepared 100 mM stock solution of taurine in deionized water. Real samples were diluted 3 to 10 fold, depending on their concentration of acidity regulators to ensure the proper pH during derivatization and yield final taurine concentrations in the linear range of the detector.

Taurine standard or real sample solutions (30 μ L) were mixed with 30 μ L of buffer (700 mM aqueous borate buffer, pH 9.3) spiked with a 30 mM concentration of 6-aminohexanoic acid as internal standard. After addition of 60 μ L of a 200 mM solution of 4-chloro-7-nitrobenzofurazan (NBD-Cl) in acetonitrile, the mixture was shaken and incubated at 45 °C for 30 minutes. Subsequently, the reaction solution was diluted 10 fold with running buffer and then applied to the reservoir of the microchip and injected and separated in triplicate.

Separations were performed on glass microchips (model T3550) from Micronit (Enschede, Netherlands) with an orthogonal channel design (10 mm x 40 mm) and a channel cross section of 20x50 μ m. The chips incorporate a double-T crossing with 100 μ m offset.

The high voltage power supply (model ECH-135L) from Micronit (Enschede, The Netherlands) has 8 programmable outputs (0-3000 V) and was additionally equipped with a custom-made trigger output (TTL) to provide a starting signal to the camera.

The chip was flushed once every three runs with running buffer (50 mM borate buffer, pH 9.3) and refilled. The voltages applied during analysis are shown in Figure 5.1.

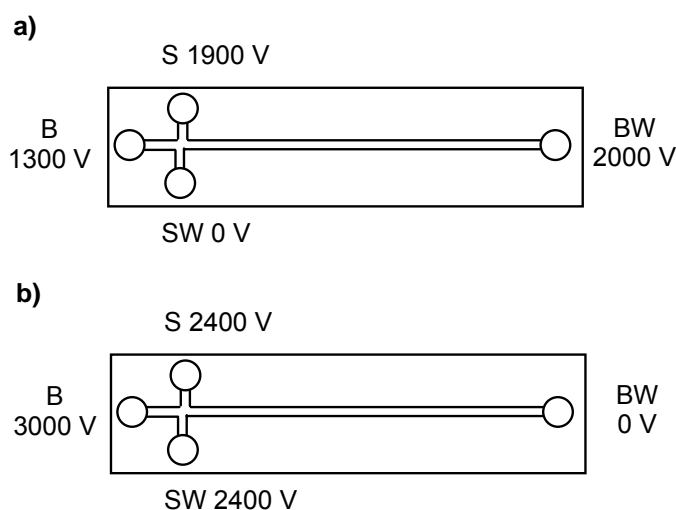


Figure 5.1: Voltage program for pinched injection (buffer reservoir (BR), buffer waste (BW), sample reservoir (SR) and sample waste (SW)) for injection a) 5 sec and separation b) 20 sec.

Separations were observed with a wavelength-resolved fluorescence detector consisting of a fluorescence microscope, a spectrograph and a CCD-camera [35]. An inverse fluorescence microscope (IX-71S1F) from Olympus (Hamburg, Germany) equipped with a xenon burner

(U-LH75XEAP0) from Olympus was used. A filter cube with components from Chroma (Rockingham, VT, USA) was employed (exciter: HQ470/40x; dichroic: 500DCLP; emitter: HQ510LP) for wavelength selection.

The triple grating turret in the spectrograph SpectraPro 308i (Acton Research, Acton, MA, USA) was provided with a 150 grooves per mm (gr/mm) grating for standard measurements, a 600 gr/mm grating for high resolution spectra and a mirror for imaging.

The light intensified CCD-camera PI-Max 512RB from Princeton Instruments (Trenton, NJ, USA) was combined with a ST133 controller ver.5 (Princeton Instruments). Data were recorded and evaluated with WinSpec/32 software version 2.5.12.0 (Princeton Instruments).

For validation purposes, the analysis was also performed on an HPLC-system with fluorescence detection. Liquid chromatographic separations and the detection were performed on the following system (all components from Shimadzu, Duisburg, Germany): two LC-10AS pumps, degasser GT-154, RF-10AXL fluorescence detector, SIL-10A autosampler, software Class LC-10 version 1.6 and CBM-10A controller unit. The injection volume was 10 μ L. A Prontosil 120-3-C18 column (Bischoff Chromatography, Leonberg, Germany) was used; particle size 3 μ m, pore size 120 Å, column dimensions 150 mm x 4.6 mm.

To ensure a sufficient retention of the highly polar analytes, a gradient of an acidic buffer (10 mM acetate, pH 5) and acetonitrile with a flow of 1 ml / minute has been used (Table 5.1). Sample preparation was performed analogous to the on-chip separation, except for the fact that the reaction solution was diluted by a factor of 100 with water prior to injection.

Table 5.1: Binary HPLC gradient; A) buffer (10 mmol, pH 5.5), B) acetonitrile.

| | 0 min | 10 min | 15 min | 19 min | 23 min | 25 min |
|---|-------|--------|--------|--------|--------|--------|
| A | 90 % | 80 % | 60 % | 10 % | 90 % | stop |
| B | 10 % | 20 % | 40 % | 90 % | 10 % | stop |

5.3 Results and discussion

The goal of this work is the quantitative determination of taurine in energy drinks and other taurine containing beverages by means of a microchip capillary electrophoretic separation with wavelength-resolved fluorescence detection. As taurine itself is neither fluorescent nor UV-active, it has to be labeled. In this work, 4-chloro-7-nitro-1,2,3-benzofurazan (NBD-Cl) is used as a reagent. The non-fluorescent NBD-Cl binds to amine functions at elevated pH-values and forms the respective NBD-derivatives, which show strong fluorescence. To improve the reproducibility of the quantitative measurements, all standard solutions and samples were spiked with 6-aminohexanoic acid as an internal standard. The use of the internal standard helps to compensate for fluctuations in the amount of injected sample, in reaction speed during derivatization, in the optical alignment of the detector and in slight changes of migration speed.

After dilution, the reaction mixture is directly filled into the sample reservoir of the microchip and injected into the separation channel. The electropherogram of a derivatized taurine standard is shown in Figure 5.2 (top left). The electropherogram shows three major peaks with peak a) being the internal standard and b) being the taurine derivative. Peak c) is a hydrolysis product of the NBD-Cl reagent, where the chloride function was exchanged with a hydroxy ion. Two very small peaks caused by yet

unidentified side products of the derivatization in front of peak a) can also be seen (*). They are apparent in all separations, but do not interfere with the quantification. The complete separation is accomplished in 12 seconds.

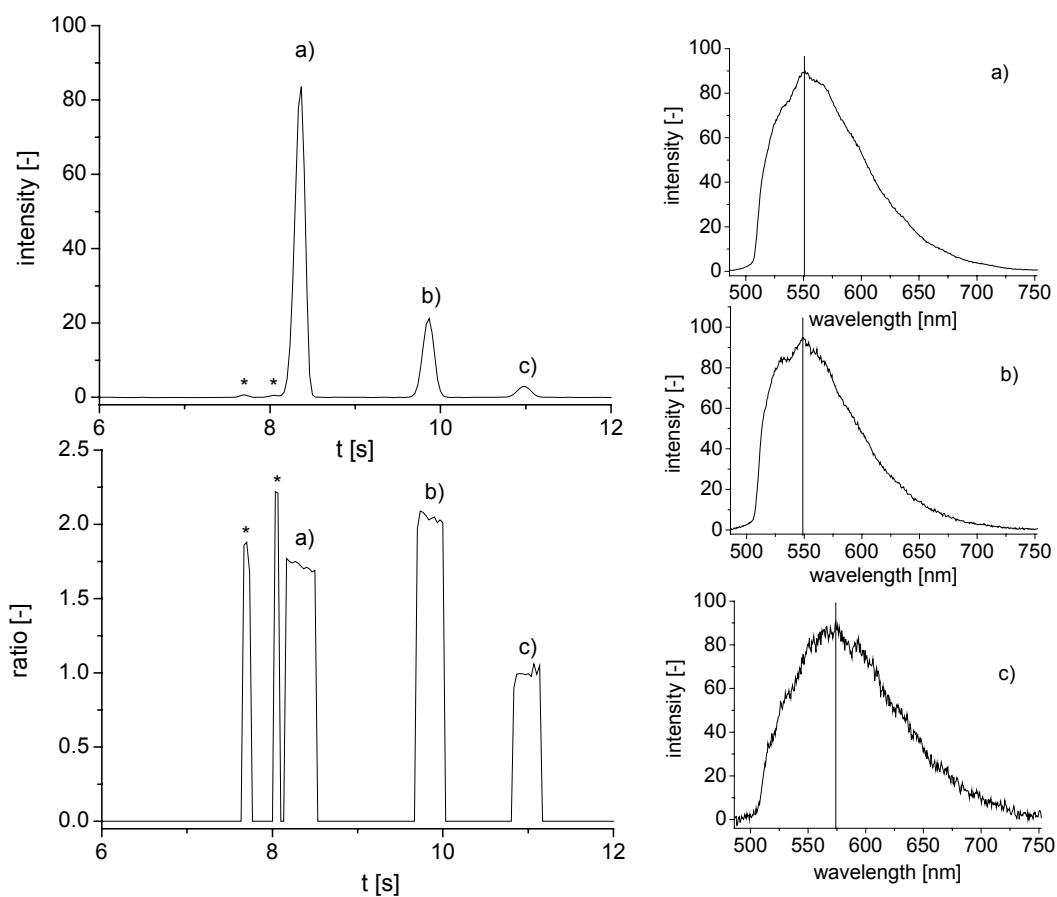


Figure 5.2: Magnification of the electropherogram of a taurine standard solution (10 mM) with corresponding peak purity plot and extracted emission spectra; a) internal standard, b) taurine derivative and c) hydrolysis product; * mark unidentified peaks.

The applied wavelength-resolved fluorescence detector set-up consists of a fluorescence microscope, a spectrograph and a CCD-camera and yields information-rich electropherograms comparable to a diode-array detector in UV/vis-spectroscopy. Figure 5.2 shows the extracted emission spectra of the three major peaks. Compared to the spectrum of the internal standard a) with an emission maximum of 551 nm, the taurine derivative b) shows a slight shift of the maximum to 548 nm and a more expressed shoulder on the left side of the curve. Even though the fluorescence in both cases is generated by the same NBD-backbone and the two molecules are very similar, subtle differences in their fluorescent properties can be detected. The third spectrum of the hydroxy derivative shows an even stronger shift of the emission maximum to 573 nm. Using the additional spectral dimension of the recorded data, possible coelutions during the separation can easily be detected by means of a peak purity plot. For this purpose, two wavelengths apparent in all observed spectra are selected (545 and 605 nm). If both measured intensities exceed a previously defined threshold value, the ratio between them is calculated and plotted (Figure 5.2 bottom left). A clean peak is then observed as a concentration independent box-shaped peak at the point of time of the original peak and the height of the calculated wavelength ratio. A coelution would show up as a strong change of ratio during one peak [35], but was not observed in these separations.

A high emphasis was set on a very simple and fast sample preparation. Standards and real samples only had to be mixed with labeling reagent and diluted twice to ensure final taurine concentrations in the linear range of the detector system. With taurine standards covering the expected concentration range of 0.1 to 50 mmol/L (before reaction and dilution), the dynamic range of the detector was found to exceed 2.5 concentration decades, yielding a straight calibration line with an R^2 value of 0.9992. Each concentration was determined in triplicate, yielding an average standard deviation of 3.4 %.

While the derivatization procedure (including an overall 40-fold dilution of the analyte for sample preparation) was not optimized for low limits of detection, the instrumental limit of quantification for the actual taurine derivative was $3 \cdot 10^{-6}$ mol/L (S/N = 10). Considering the injection volume of approximately 60 pL, the smallest detectable amount of the taurine derivative (S/N = 3) actually injected into the separation channel was as low as 60 amol, corresponding to a concentration of $1 \cdot 10^{-6}$ mol/L.

Eleven energy drinks and other taurine containing beverages were purchased (Table 5.2) and analyzed analogous to the taurine standard solutions. Whereas most of the energy drinks exploit the legal limit of 0.4% (31.96 mmol/L) taurine content, mixed beverages based on tap water, fruit juice and also beer were found in the lower concentration range from 0.8 to 3 mmol/L. No taurine containing beverages with a medium concentration around 10-20 mmol/L could be found and used for this analysis.

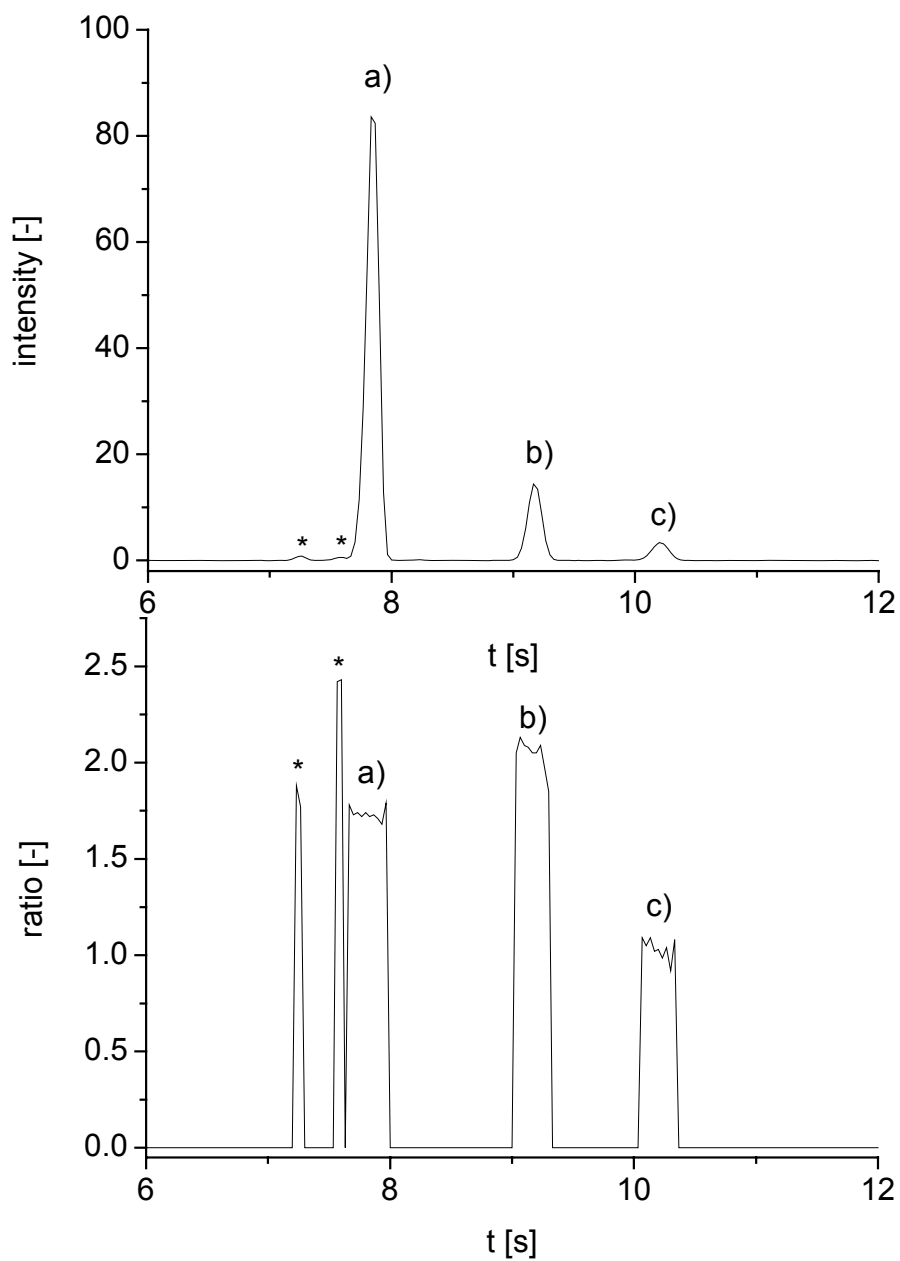


Figure 5.3: Electropherogram of a taurine real sample (Red Bull Sugar Free) with corresponding peak purity plot; a) internal standard, b) taurine derivative and c) hydrolysis product; * mark unidentified peaks.

Figure 5.3 shows a typical electropherogram of a derivatized energy drink sample along with its peak purity plot. Comparable to the taurine standard solutions, the data shows no sign of coelution. All results generated by the on-chip analysis were compared with the supplier's information and found to be in good accordance (Table 5.2). The average standard deviation for all real sample measurements was 3.0 %.

Table 5.2: Results of taurine content determined by HPLC and on-chip CE compared with the suppliers information.

| Beverage | C_{taurine} (supplier) [mmol/L] | C_{taurine} (MCE) [mmol/L] | C_{taurine} (HPLC) [mmol/L] |
|------------------------|---|--|---|
| Red Bull | 31.96 | 31.92 | 30.27 |
| Red Bull sugar free | 31.96 | 31.52 | 31.24 |
| Mr. Energy | 31.96 | 32.02 | 30.85 |
| Caps energy | n/a | 3.19 | 2.68 |
| Effect | 31.96 | 31.89 | 31.29 |
| S1 | 31.96 | 33.49 | 32.19 |
| Veltins V+ energy beer | n/a | 1.85 | 1.45 |
| Kick off (bottle) | 31.96 | 33.78 | 32.81 |
| Kick off (can) | 2.40 | 3.26 | 2.68 |
| Xi energy water | 0.80 | 1.01 | 0.87 |
| Xi climax | 31.96 | 32.02 | 31.27 |

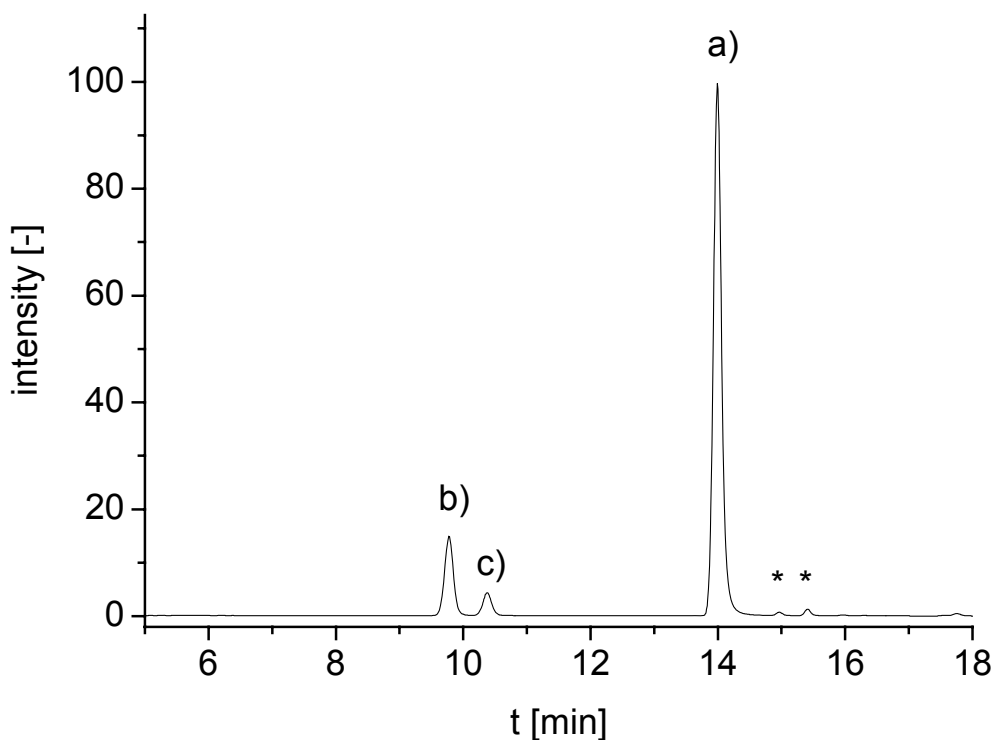


Figure 5.4: HPLC chromatogram of taurine standard solution (10 mM); a) internal standard, b) taurine derivative and c) hydrolysis product; * mark unidentified peaks.

To validate the results of the microchip separation, the analysis was also performed on a commercially available HPLC system with fluorescence detection. Using a column with C18 material, the aqueous part of the acetonitrile/water gradient had to be acidified (10 mM acetate, pH 5) to ensure enough retention of the highly polar NBD-derivatives. Figure 5.4 shows the liquid chromatogram of a derivatized energy drink sample. In contrast to the electrophoresis, the chromatographic separation with its different retention mechanism results in a changed elution order of the three

major peaks. The analytes are separated after 15 minutes; one complete run takes 23 minutes. Threefold injection of the diluted reaction mixtures yielded average standard deviations of 1.8 %. The resulting taurine concentrations determined by means of HPLC are in good agreement with the on-chip measurements and the supplier's information (Table 5.2). Both detection methods delivered very similar results, which is obvious from the correlation plot (Figure 5.5).

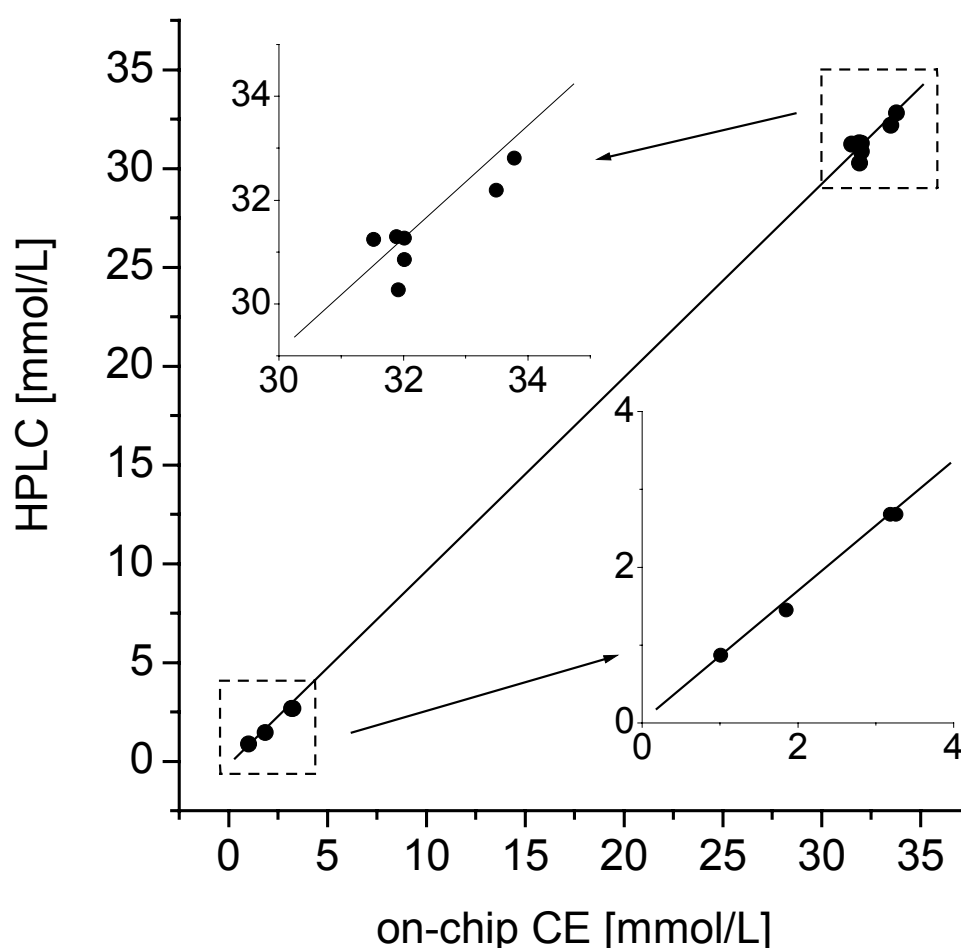


Figure 5.5: Correlation plot of HPLC and MCE results of real sample measurements. Lower and higher concentration ranges have been enlarged in the inserts.

5.4 Conclusion

This work demonstrates the development of a method for the quantitative on-chip determination of taurine in energy drinks and other taurine containing beverages. After derivatization with NBD-Cl, the sample is filled into the reservoir of a glass microchip and separated by capillary electrophoresis. Three major peaks, the internal standard, the taurine derivative and the hydrolysis product of the reagent are separated in only 12 seconds. The separation is observed with a wavelength-resolved fluorescence detector consisting of a fluorescence microscope, a spectrograph and an intensified CCD-camera. The yielded information-rich electropherogram shows even subtle differences in the fluorescent properties of the observed analytes. Furthermore, it enables peak purity calculations, ensuring that no hidden coelution is taking place. Including only dilution and addition of the labeling reagent, a very fast and straightforward sample preparation method was applied, which was adapted to the anticipated taurine concentrations in real samples. A calibration curve with standards covering the expected concentration range from 0.1 to 50 mmol/L was recorded. The smallest detectable amount ($S/N = 3$) of taurine derivative actually injected into the separation channel was 60 amol, corresponding to a concentration of $1 \cdot 10^{-6}$ mol/L. The method was successfully validated by liquid chromatography with fluorescence detection.

5.5 References

- [1] S. C. Terry, *IEEE Trans. Electron Devices*, **1979**, 26, 1880-1886.
- [2] A. Manz, N. Graber, H. M. Widmer, *Sens. Actuators, B*, **1990**, 1, 244-248.
- [3] D. J. Harrison, A. Manz, Z. Fan, H. Lüdi, H. M. Widmer, *Anal. Chem.*, **1992**, 64, 1926-1932.
- [4] A. Ros, W. Hellmich, T Duong, D. Anselmetti, *J. Biotechnol.*, **2004**, 112, 65-72.
- [5] S. C. Jacobsen, L. B. Koutny, R. Hergenröder, A. W. Moore, J. M. Ramsey, *Anal. Chem.*, **1994**, 66, 3472-3476.
- [6] W. Hellmich, C. Pelargus, K. Leffhalm, A. Ros, D. Anselmetti, *Electrophoresis*, **2005**, 26, 3689-3696.
- [7] N. Piehl, M. Ludwig, D. Belder, *Electrophoresis*, **2004**, 25, 3848-3852.
- [8] G. M. Greenway, S. J. Haswell, P. H. Petsul, *Anal. Chim. Acta*, **1999**, 387, 1-10.
- [9] N. Malcik, J. P. Ferrance, J. P. Landers, P. Caglar, *Sens. Actuators, B*, **2005**, 107, 24-31.
- [10] E. X. Vrouwe, R. Luttge, W. Olthuis, A. van den Berg, *Electrophoresis*, **2005**, 26, 3032-3042.
- [11] C. D. Garcia, G. Engling, P. Herckes, J. L. Collett, C. S. Henry, *Environ. Sci. Technol.*, **2005**, 39, 618-623.

- [12] J. Wang, J. Zima, N. S. Lawrence, M. P. Chatrathi, A. Mulchandani, G. E. Collins, *Anal. Chem.*, **2004**, *76*, 4721-4726.
- [13] S. A. Pasas, N. A. Lacher, M. I. Davies, S. M. Lunte, *Electrophoresis* **2002**, *23*, 759-766.
- [14] M. Macka, P. Andersson, P. R. Haddad, *Anal. Chem.*, **1998**, *70*, 743-749.
- [15] A. Oki, Y. Takamura, Y. Ito, Y. Horiike, *Electrophoresis*, **2002**, *23*, 2860-2864.
- [16] I. Rodriguez, N. Chandrasekhar, *Electrophoresis*, **2005**, *26*, 1114-1121.
- [17] D. Belder, M. Ludwig, *Electrophoresis*, 2003, *24*, 3595-3606.
- [18] N. J. Petersen, R. P. H. Nikolajsen, K. B. Mogensen, J. P. Kutter, *Electrophoresis*, **2004**, *25*, 253-269.
- [19] J. Milei, R. Ferreira, S. Llesuy, P. Forcada, J. Covarrubias, A. Boveris, *Am. Heart J.*, **1992**, *123*, 339-345.
- [20] R. J. Huxtable, L. A. Sebring, *Trends Pharmacol. Sci.*, **1986**, *7*, 481-485.
- [21] R. J. Huxtable, *Physiol. Rev.*, **1992**, *72*, 101-163.
- [22] S. G. Hartley, H. O. Goodman, Z. Shihabi, *Neurochem. Res.*, **1989**, *14*, 149-152.
- [23] S. K. Bhatnagar, J. D. Welty, A. R. Al Yussuf, *Int. J. Cardiol.*, **1990**, *27*, 361-366.

- [24] G. E. Gray, A. M. Landel, M. M. Meguid, *Nutrition*, **1990**, *10*, 11-15.
- [25] G. B. Schuller-Levis, E. Park, *FEMS Microbiol. Lett.*, **2003**, *226*, 195-202.
- [26] T. R. I. Cataldi, G. Telesca, G. Bianco, D. Nardiello, *Talanta*, **2004**, *64*, 626-630.
- [27] S. Muo, X. Ding, Y. Liu, *J. Chromatogr., B: Biomed. Appl.*, **2002**, *781*, 251-267.
- [28] C. J. Waterfield, *J. Chromatogr., B: Biomed. Appl.*, **1994**, *657*, 37-45.
- [29] Z. Chen, G. Xu, K. Specht, R. Yang, S. She, *Anal. Chim. Acta*, **1994**, *296*, 249-253.
- [30] T. Sakai, T. Nagasawa, *J. Chromatogr.*, **1992**, *576*, 155-157.
- [31] G. P. McMahon, R. O'Kennedy, M. T. Kelly, *J. Pharm. Biomed. Anal.*, **1996**, *14*, 1287-1294.
- [32] F. Qu, Z. Qi, K. Liu, S. Mou, *J. Chromatogr., B: Biomed. Appl.*, **1999**, *730*, 161-166.
- [33] M. T. Kelly, H. Fabre, D. Perett, *Electrophoresis*, **2000**, *21*, 699-705.
- [34] X. Zhang, J. N. Stuart, J. V. Sweedler, *Anal. Bioanal. Chem.*, **2002**, *373*, 323-343.
- [35] S. Götz, U. Karst, *Sens. Actuators, B*, **2007**, in press
DOI:10.1016/j.snb.2006.08.027.

Chapter 6

Bilayer Vesicles of Amphiphilic Cyclodextrins: Host Membranes that Recognize Guest Molecules[‡]

A family of amphiphilic cyclodextrins has been prepared through 6-S-alkylation (alkyl = n-dodecyl and n-hexadecyl) of the primary side and 2-O-PEGylation of the secondary side of α -, β - and γ -cyclodextrin. These cyclodextrins form non-ionic bilayer vesicles in aqueous solution. Molecular recognition of a hydrophobic anion (adamantane carboxylate) by the cyclodextrin vesicles was investigated using capillary electrophoresis, exploiting the increase in electrophoretic mobility that occurs when the hydrophobic anions bind to the non-ionic cyclodextrin vesicles. It was found that in spite of the presence of oligo(ethylene glycol) substituents, the β -cyclodextrin vesicles retain their characteristic affinity for adamantane carboxylate ($K_a = 7.1 \times 10^3 M^{-1}$), whereas γ -cyclodextrin vesicles have less affinity ($K_a = 3.2 \times 10^3 M^{-1}$), and α -cyclodextrin or non-cyclodextrin, non-ionic vesicles have very little affinity ($K_a \sim 100 M^{-1}$). Specific binding of the adamantane carboxylate to β -cyclodextrin vesicles was also evident in competition experiments with β -cyclodextrin in solution. Hence, the

cyclodextrin vesicles can function as host bilayer membranes that recognize small guest molecules by specific non-covalent interaction.

‡This chapter is based on: P. Falvey, C.W. Lim, R. Darcy, T. Revermann, U. Karst, M. Giesbers, A.T.M. Marcelis, A. Lazar, A.W. Coleman, D.N. Reinhoudt, B.J. Ravoo, *Chem. Eur. J.* **2005**, *11*, 1171-1180. Additional information regarding amphiphilic vesicles synthesis, characterization of the cyclodextrin species, vesicle preparation, dye encapsulation, dynamic light scattering, x-ray diffraction analysis, langmuir plots and transmission electron spectroscopy is part of this comprehensive publication.

6.1 Introduction

Amphiphilic cyclodextrins are cyclic oligo(α -(1,4)-glucopyranosides) modified with hydrophobic and hydrophilic substituents that aggregate into a variety of lyotropic phases in water [1-10]. The hydrophobic groups drive hydrophobic aggregation of the amphiphiles, while the hydrophilic groups are required to guarantee sufficient water solubility. The type and stability of the lyotropic phases critically depend on the nature and number of hydrophobic and hydrophilic substituents, the balance between hydrophobic and hydrophilic groups, and factors such as temperature, concentration, and ionic strength. A particularly interesting example of aggregation of amphiphilic cyclodextrins in water is the formation of bilayer vesicles composed entirely of (modified) cyclodextrins. Cyclodextrin vesicles consist of bilayers of cyclodextrins, in which the hydrophobic 'tails' are directed inwards and the hydrophilic macrocycle 'head groups' are facing water, enclosing an aqueous interior (Figure 6.1 A and B). Recently vesicles composed entirely of non-ionic [11-14], anionic [15] and cationic [16] amphiphilic cyclodextrins have been described.

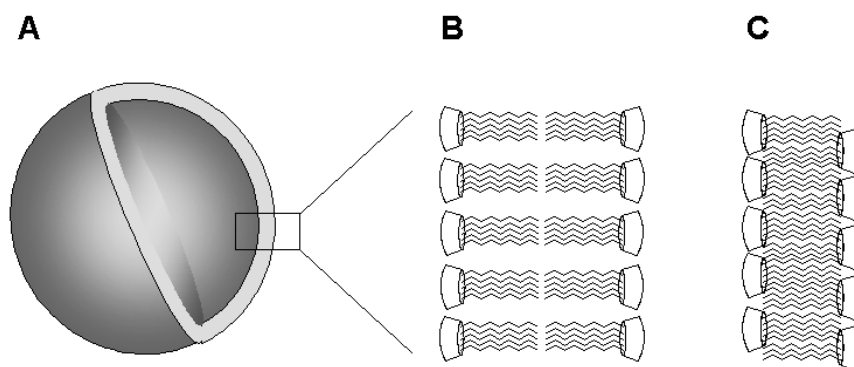


Figure 6.1: Cyclodextrin vesicles consist of bilayers of cyclodextrins (in which the hydrophobic ‘tails’ are directed inwards and hydrophilic macrocycle ‘head groups’ are facing water) enclosing an aqueous interior. (A) Schematic representation of a unilamellar vesicle. (B) Illustration of an extended, all-trans packing of the alkyl chains in a cyclodextrin bilayer. (C) Illustration of an interdigitated packing of the alkyl chains in a cyclodextrin bilayer.

Cyclodextrin vesicles combine the properties of liposomes and macrocyclic host molecules in their potential to encapsulate water-soluble molecules in the aqueous interior, to absorb hydrophobic molecules in the bilayer membrane, and finally to recognize and bind specific types of guest molecules through inclusion in the cyclodextrin cavities at the surface of the

vesicle. The recognition of small guest molecules by cyclodextrin hosts assembled in a bilayer membrane is a useful model of recognition of substrates or ligands by receptors on the surface of cell membranes. In nature many recognition processes at the cell surface are amplified in affinity and selectivity by multivalent interactions [17, 18].

Here, a family of amphiphilic cyclodextrins that form stable non-ionic vesicles in water is described in detail. Cyclodextrins of various ring sizes (α -, β - and γ -cyclodextrin, with 6, 7 and 8 glucose units, respectively) were modified with hydrophobic *n*-dodecyl and *n*-hexadecyl and hydrophilic oligo(ethylene glycol) substituents (Figure 6.2). The properties of vesicles of these cyclodextrins were studied, with an emphasis on capillary electrophoretic methods. The inclusion of a small guest molecule (adamantane carboxylate) in the cyclodextrin cavities at the surface of the vesicle is examined. When the negatively charged guest binds to a nonionic vesicle, the occurring change in electrophoretic mobility is measured and used to calculate the respective binding constants.

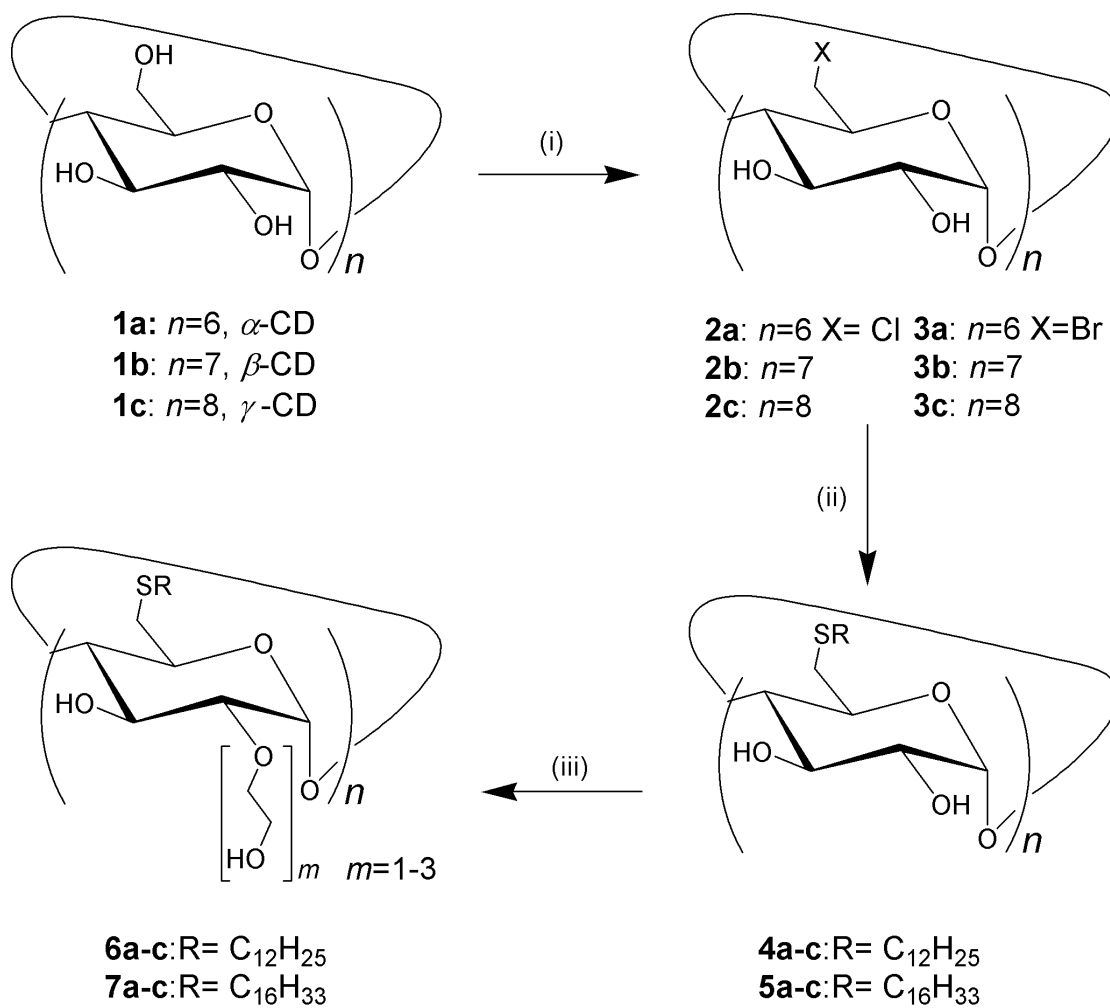


Figure 6.2: Synthesis of amphiphilic cyclodextrins. Reaction conditions: (i) CH₃SO₂Cl, DMF, 65 °C, 2 days (to give chlorides **2a-2c**) or NBS, Ph₃P, DMF, 60 °C, 4 h (to give bromides **3a-3c**). (ii) *t*-BuOK or NaH, RSH, DMF, 80 °C, 3-4 days. (iii) Ethylene carbonate, K₂CO₃, *N,N,N',N'*-tetramethyl urea, 150 °C, 4 h.

6.2 Materials and Methods

Capillary electrophoresis was carried out as described previously [13, 19]. Measurements were carried out on a 57 cm (48.5 cm from inlet to detector) fused-silica capillary (75 μm internal diameter; Polymicro Technologies, Phoenix, AZ) with a separation voltage of 25 kV, using an Agilent HP ^{3D}CE system. The capillary was conditioned with 1 M NaOH (5 min), water (1 min), 10 mM phosphate buffer (1 min) before each series of measurements and running buffer (1 min) before each measurement. The running buffer was prepared with a varying concentration of adamantane carboxylate in 10 mM phosphate buffer adjusted to pH 7.5. The analyte sample (0.2 mg mL⁻¹ in 5 mM phosphate buffer) was introduced with 34.5 mbar injection for 5 s and detected with a diode-array detector at 200 nm. Measurements were repeated 2 or 3 times for each concentration. For competition experiments, the elution time of the vesicles was determined in the presence of a known concentration (0.5, 1.0 and 5.0 mM) of β -cyclodextrin **1b** (Figure 6.2) and various concentrations of adamantane carboxylate in the capillary. The electrophoretic mobility μ_{ep} of the vesicles was determined from the migration time according to the following equation:

$$\mu_{ep} = l \cdot L \cdot V^{-1} \cdot (1/t - 1/t_{eof})$$

l and L denote the effective length (in m) of the capillary from injector to detector and the total length respectively, V is the voltage (in V), and t_{eof} and t represent the migration times (in s) of the electroosmotic flow (detected by a negative peak) and the sample, respectively. Binding constants K_a were calculated from a non-linear regression of the change of electrophoretic mobility of the vesicles as a function of the adamantane carboxylate concentration, assuming that the concentration of complexed guest is always small relative to the total guest concentration [19].

6.3 Results and Discussion

Given that all amphiphilic cyclodextrins described above form bilayer vesicles in water, is it possible to bind small guest molecules in the cyclodextrin cavities at the surface of these vesicles? Adamantane carboxylate - like all adamantanes - is known to be a good guest for inclusion into β -cyclodextrin **1b** (Figure 6.2) ($K_a = 3.2 \times 10^4 \text{ M}^{-1}$ at pH 7.2 and 25 °C) while it has much weaker interaction with γ -cyclodextrin **1c** (Figure 6.2) ($K_a = 5.0 \times 10^3 \text{ M}^{-1}$) and even less with α -cyclodextrin **1a** (Figure 6.2) ($K_a = 2.3 \times 10^2 \text{ M}^{-1}$) [20, 21]. The inclusion interaction of this typical guest with the cyclodextrin host vesicles was investigated using capillary electrophoresis. This technique exploits the difference in electrophoretic mobility between free host and host-guest complex (or free guest and host-guest complex) to quantify host-guest interactions [22, 23]. Capillary electrophoresis has proven particularly useful to quantify the interaction between β -cyclodextrin and anionic guests [19] as well as β -cyclodextrin vesicles and anionic guests in dilute aqueous solution. Here, the electrophoretic mobility of the host vesicles of **6a-6c** (Figure 6.2) was measured in the presence of increasing concentration of adamantane carboxylate in the background electrolyte (Figure 6.3). There is some precedent for the investigation of liposomes using capillary electrophoresis [24-29].

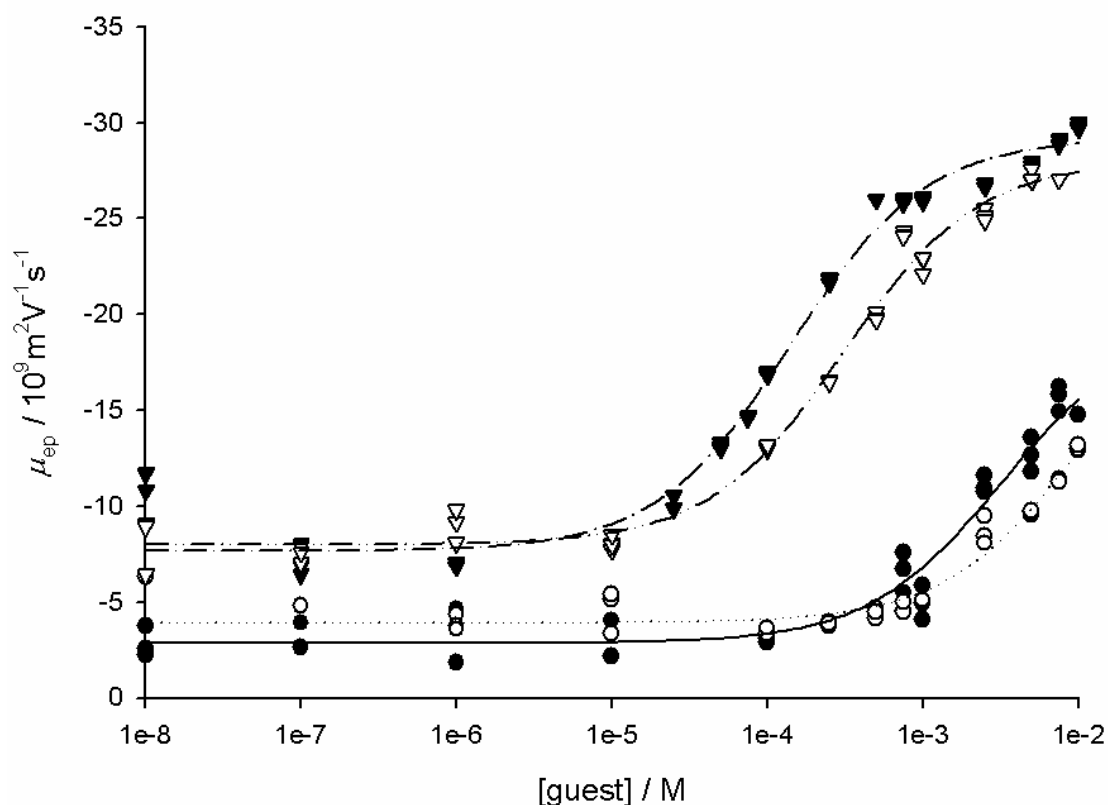


Figure 6.3: Electrophoretic mobility (μ_{ep}) of vesicles in the presence of adamantane carboxylate guest. Legend: \circ : α -cyclodextrin vesicles (**6a**); \blacktriangledown : β -cyclodextrin vesicles (**6b**); ∇ : γ -cyclodextrin vesicles (**6c**); \bullet : $C_{12}EO_3$ reference vesicles.

All cyclodextrin vesicles as well as the $C_{12}EO_3$ reference vesicles invariably have significant negative electrophoretic mobility ($\mu_{ep} \sim -8 \times 10^{-9} \text{ m}^2 \text{ V}^{-1} \text{ s}^{-1}$) at neutral pH in dilute buffer solution. The negative electrophoretic mobility most likely results from a preferential absorption of hydroxyl anions at the interface between PEGylated cyclodextrin vesicles and bulk aqueous solution [30, 31]. For an electrophoretic mobility of $-8 \times 10^{-9} \text{ m}^2 \text{ V}^{-1} \text{ s}^{-1}$ and a vesicle diameter of 160 nm, the Smoluchovski equation predicts a Zeta

potential of -11 mV. In the presence of excess adamantane carboxylate, vesicles of **6b** and **6c** (Figure 6.2) have an electrophoretic mobility of ca. $-30 \times 10^{-9} \text{ m}^2 \text{ V}^{-1} \text{ s}^{-1}$, which would imply a Zeta potential of ca. -42 mV.

The increase of electrophoretic mobility of the host vesicles in the presence of increasing concentration of guest was analyzed in terms of the formation of a 1:1 inclusion complex of **6a-6c** (Figure 6.2) and adamantane carboxylate, characterized by the association constant K_a . The results are summarized in Table 6.1. As anticipated, vesicles of the β -cyclodextrin amphiphile **6b** (Figure 6.2) have the highest binding constant $K_a = 7.1 \times 10^3 \text{ M}^{-1}$. This is significantly lower than for β -cyclodextrin **1b** (Figure 6.2). The difference might be attributed to some hindrance of inclusion into the cavity of **6b** (Figure 6.2) due to the presence of oligo(ethylene glycol) residues or a degree of anti-cooperativity due to the increasing presence of anionic guests on the vesicle surface. However, the Scatchard plot has a linear slope and an abscissa intercept very close to 1.0, proving the presence of identical and independent binding sites on the vesicle surface. The inferior binding constant for **6b** (compared to **1b**) (Figure 6.2) can therefore be ascribed to some steric hindrance and some reduction in the hydrophobicity of the host by the oligo(ethylene glycol) residues. This is consistent with the observation that non-amphiphilic, PEGylated cyclodextrins also are poorer hosts than native cyclodextrins are [32].

Table 6.1: Binding constants K_a of adamantane carboxylate to vesicles in 10 mM phosphate buffer (pH 7.5) at 25°C.

| vesicle | K_a [M^{-1}] |
|--------------|---------------------------|
| 6a | 96 ± 40 |
| 6b | $7.1 \pm 0.6 \times 10^3$ |
| 6c | $3.2 \pm 0.3 \times 10^3$ |
| $C_{12}EO_3$ | $3.1 \pm 0.6 \times 10^2$ |

Compared to vesicles of **6b**, vesicles of **6c** (Figure 6.2) have considerably less affinity for adamantane carboxylate ($K_a = 3.0 \times 10^3 M^{-1}$), reflecting the lower affinity of a γ -cyclodextrin cavity relative to that of a β -cyclodextrin to form inclusion complexes with this guest. Also, one expects steric hindrance and reduction in the hydrophobicity of the host by the oligo(ethylene glycol) residues. For host **6c** (Figure 6.2) the formation of 1:2 host-guest complexes, particularly at high guest concentrations, cannot be excluded. However, the Scatchard plot again has a linear slope and an abscissa intercept very close to 1.0.

The association constant of vesicles of **6a** (Figure 6.2) with adamantane carboxylate ($K_a = 96 M^{-1}$) is very small compared to that of **6b** and **6c** (Figure 6.2), reflecting the fact that the cavity of α -cyclodextrin is too narrow to be a good host for adamantane guests. In fact, the affinity of **6a** (Figure 6.2) is

comparable to that of the reference vesicles of $C_{12}EO_3$, lacking any specific host cavities. The increase in electrophoretic mobility of vesicles of **6a** (Figure 6.2) and $C_{12}EO_3$ in the presence of high concentrations of adamantane carboxylate (> 1 mM) more likely results from partitioning of the hydrophobic anion from aqueous solution into the hydrophobic bilayer.

To confirm the specific and reversible binding of adamantane carboxylate to vesicles of **6b** (Figure 6.2), competition experiments were carried out in the presence of β -cyclodextrin **1b** (Figure 6.2). To this end, the electrophoretic mobility of vesicles of **6b** (Figure 6.2) was determined in the presence of a given concentration (0.5, 1.0 and 5.0 mM) of **1b** (Figure 6.2) and various concentrations of adamantane carboxylate in the capillary (Figure 6.4).

The association constant K_a of adamantane carboxylate to cyclodextrin **6b** (Figure 6.2) was calculated using the concentration of free adamantane carboxylate calculated from the total concentration after subtraction of adamantane carboxylate complexed with **1b** (Figure 6.2), as calculated from their binding constant ($K_a = 3.2 \times 10^4 \text{ M}^{-1}$). As can be readily deduced from Figure 6.4 and Table 6.2, a similar binding constant was obtained from each competition experiment. These results demonstrate that capillary electrophoresis provides reliable quantitative information about these dynamic equilibria.

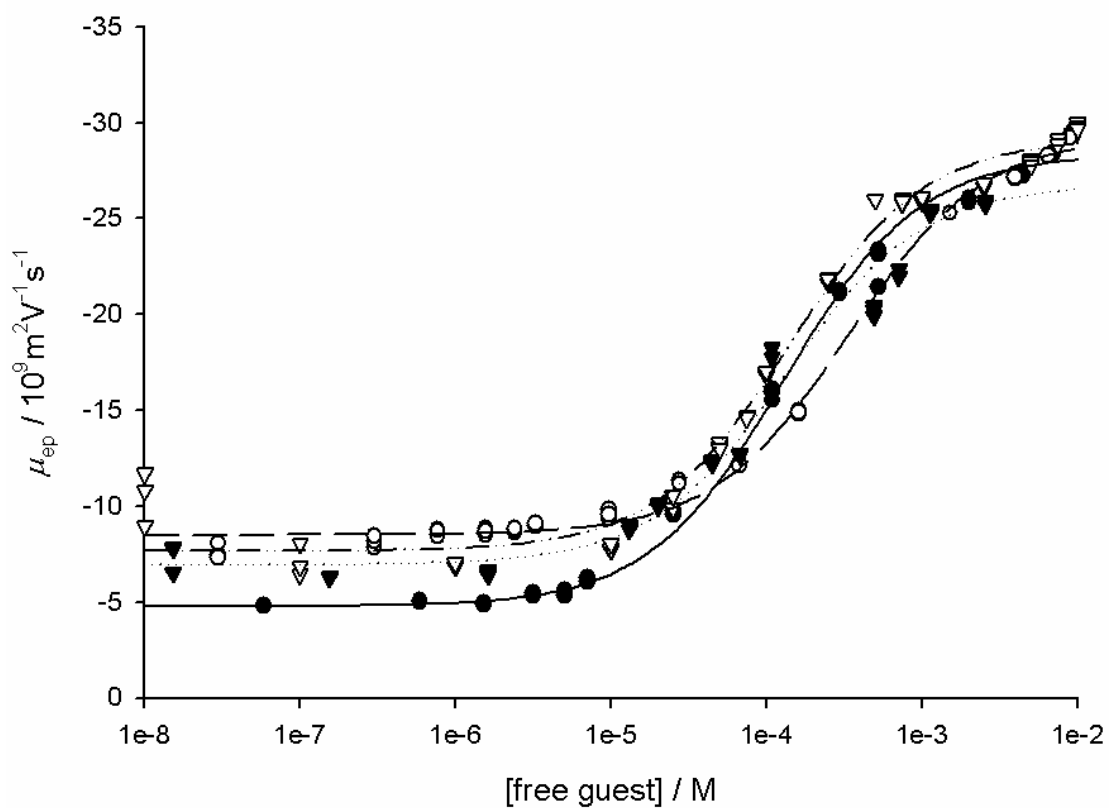


Figure 6.4: Electrophoretic mobility (μ_{ep}) of β -cyclodextrin vesicles (**6b**) (Figure 6.2) in the presence of adamantane carboxylate guest and competing β -cyclodextrin host (**1b**). Legend: ∇ : 0 mM; \bullet : 0.5 mM; \circ : 1 mM; \blacktriangledown : 5 mM.

Table 6.2: Binding constants K_a of adamantane carboxylate to β -cyclodextrin vesicles (**6b**) obtained from competition experiments in the presence of β -cyclodextrin (**1b**).

| β -cyclodextrin [mM] | K_a [M^{-1}] |
|----------------------------|---------------------------|
| 0 | $7.1 \pm 0.6 \times 10^3$ |
| 0.5 | $7.7 \pm 0.5 \times 10^3$ |
| 1.0 | $3.0 \pm 0.2 \times 10^3$ |
| 5.0 | $7.4 \pm 0.9 \times 10^3$ |

6.4 Conclusions

Bilayer vesicles formed by non-ionic amphiphilic cyclodextrins function as host membranes that bind suitable guest molecules by hydrophobic inclusion at their surface. Capillary electrophoresis provides quantitatively reliable information about these dynamic interactions at the membrane surface. The cyclodextrin cavities function as independent host sites and their characteristic affinity and selectivity for a given guest molecule is not affected when they are confined to a hydrophobic bilayer membrane. The recognition of small guest molecules by cyclodextrin hosts assembled in a bilayer membrane is a useful model of recognition of substrates and ligands by receptors on the surface of cell membranes. In future work, the multivalent interaction of oligomeric guest molecules with host molecules at the vesicle surface will be investigated. Critical parameters will be the density and mobility of the host in the membrane, the number and flexibility of binding moieties on the guest, and the presence of monovalent competitors. It is aimed to exploit these specific interactions to bind molecules to vesicles, vesicles to vesicles and vesicles to surfaces. It will be investigated, whether these interactions of cyclodextrin vesicles can be used to form a custom-made quasi-stationary phase for capillary electrophoretic separations. The feasibility of developing a separation method for different vesicle sizes will be examined.

6.5 References

- [1] R. C. Petter, J. S. Salek, C. T. Sikorski, G. Kumaravel, Lin, F. T., *J. Am. Chem. Soc.* **1990**, *112*, 3860-3868.
- [2] H. Parrot-Lopez, C.-C. L., P. Zhang, A. Baszkin, G. Albrecht, C. de Rango, A. W. Coleman, *J. Am. Chem. Soc.* **1992**, *114*, 5479-5480.
- [3] A. Schalchli, J. J. Benattar, P. Tschoreloff, P. Zhang, Coleman, A. W., *Langmuir* **1993**, *9*, 1968-1970.
- [4] P. C. Tschoreloff, M. M. Boissonnade, A. W. Coleman, Baszkin, A., *Langmuir* **1995**, *11*, 191-196.
- [5] M. Skiba, D. Duchêne, F. Puisieux, D. Wouessidjewe, *Int. J. Pharm.* **1996**, 113-121.
- [6] A. Gulik, H. Delacroix, D. Wouessidjewe, M. Skiba, *Langmuir* **1998**, 1050-1057.
- [7] R. Auzély-Velty, F. Djedaïni-Pilard, S. Désert, B. Perly, T. Zemb, *Langmuir* **2000**, *16*, 3727-3734.
- [8] R. Auzély-Velty, C. Péan, F. Djedaïni-Pilard, T. Zemb, B. Perly, *Langmuir* **2001**, 504-510.
- [9] A. Mazzaglia, B. J. Ravoo, R. Darcy, P. Gambadauro, F. Mallamace, *Langmuir* **2002**, *18*, 1945-1948.
- [10] D. Lombardo, A. Longo, R. Darcy, Mazzaglia, A., *Langmuir* **2004**, *20*, 1057-1062.
- [11] B. J. Ravoo, R. Darcy, *Angew. Chem.* **2000**, *112*, 4494-4496.

- [12] D. Nolan, R. Darcy, Ravoo, B. J., *Langmuir* **2003**, 4469-4472.
- [13] B. J. Ravoo, J. C. Jacquier, G. Wenz, *Angew. Chem. Int. Ed.* **2003**, *42*, 2066-2070.
- [14] A. Mazzaglia, D. Forde, D. Garozzo, P. Malvagna, B. J. Ravoo, R. Darcy, *Org. Biomol. Chem.* **2004**, 957-960.
- [15] T. Sukegawa, T. Furuike, K. Niikura, A. Yamagishi, K. Monde, S.-I. Nishimura., *Chem. Commun.* **2002**, 430-431.
- [16] R. Donohue, A. Mazzaglia, B. J. Ravoo, R. Darcy, *Chem. Commun.* **2002**, 2864-2865.
- [17] M. Mammen, S.-K. Choi, G. M. Whitesides, *Angew. Chem. Int. Ed.* **1998**, *37*, 2754-2794.
- [18] L. L. Kiessling, J. E. Gestwicki, L. E. Strong, *Curr. Opin. Chem. Biol.* **2000**, *4*, 696-703.
- [19] B. J. Ravoo, J.-C. Jacquier, *Macromolecules* **2002**, *35*, 6412-6416.
- [20] W. C. Cromwell, K. Byström, M. R. Eftink, *J. Phys. Chem.* **1985**, *89*, 326-332.
- [21] M. Weickenmeier, G. Wenz, *Macromol. Rapid Commun.* **1996**, *17*, 731-736.
- [22] I. J. Colton, J. D. Carbeck, J. Rao, Whitesid, G. M., M. Weickenmeier, G. Wenz, *Macromol. Rapid Commun.* **1996**, *17*, 731-736.
- [23] I. J. Colton, J. D. Carbeck, J. Rao, Whitesid, G. M., M. Weickenmeier, G. Wenz, *Electrophoresis* **1998**, *19*, 367-382.
- [24] M. A. Roberts, L. Locascio-Brown, W. A. MacCrehan, R. A. Durst, *Anal. Chem.* **1996**, *68*, 3434-3440.

- [25] K. Kawakami, Y. Nishihara, Hirano, K., *Langmuir* **1999**, *15*, 1893-1895.
- [26] S. K. Wiedmer, J. Hautala, J. M. Holopainen, P. K. J. Kinnunen, M. L. Riekkola, *Electrophoresis* **2001**, *22*, 1305-1313.
- [27] C. F. Duffy, S. Gafoor, D. P. Richards, H. Admadzadeh, R. O'Kennedy, E. A. Arriaga, *Anal. Chem.* **2001**, *73*, 1855-1861.
- [28] A. N. Phayre, H. M. V. Farfano, M. A. Hayes, *Langmuir* **2002**, *18*, 6499-6503.
- [29] J. McKeon, M. G. Khaledi, *J. Chromatography A* **2003**, *1004*, 39-46.
- [30] Y. H. M. Chan, R. Schweiss, C. Werner, M. Grunze, *Langmuir* **2003**, *19*, 7380-7385.
- [31] M. Johnsson, A. Wagenaar, J. B. F. N. Engberts, *J. Am. Chem. Soc.* **2003**, *125*, 757-760.
- [32] I. N. Topchieva, P. Mischnick, G. Kühn, V. A. Polyakov, S. V. Elezkaya, G. I. Bystryzky, K. I. Karezin, B. C., *Bioconjugate Chem.* **1998**, *9*, 676-682.

Chapter 7

Concluding remarks and future perspectives

In this work, microchip capillary electrophoresis (MCE) has proven to be a valuable tool for quantitative analysis. Novel analytical instrumentation and new methods for the determination of analytes in real samples using MCE have been developed.

Future improvements in quantitative microchip analysis need to include further development of the required devices and analytical strategies. Many working steps, which have been performed manually in this thesis, can be automated, e.g. the flushing and the filling of the microchip. Thus, experimental errors can be reduced, and higher precision will be obtained. Some handling related errors like positioning of the microchip on the detector could be omitted as well. This way, the cycle times of analysis can be adjusted to the very short separation times, which have been reported in this thesis.

The development of integrated microfluidic devices will save labor and reduces the number of interconnections between different devices. For the

analysis of real samples in this thesis, the construction of a microchip, which incorporates the derivatization reaction on the same chip, would be advantageous. Then, only the original sample and some reagents have to be brought to the chip and all further reaction and separation steps can be automated. Because of that, the total analysis time will be reduced as on-chip reactions and separations tend to be faster than in standard lab scale. Furthermore, the sample preparation step is directly coupled to the analysis and therefore standardized and sources of potential errors caused by users would be eliminated. For some applications like portable instruments, dedicated combinations of chip and support instrumentation could be the method of choice.

Summary

The development of novel instrumentation and analytical methodology for quantitative microchip capillary electrophoresis (MCE) is described in this thesis. Demanding only small quantities of reagents and samples, microfluidic instrumentation is highly advantageous. Fast separations at high voltages have been performed, which require the use of flexible high-voltage power supplies that have been developed in this work.

An introductory overview of the general requirements of MCE is provided. Differences of chip-based CE and conventional CE are addressed, and the effects of buffer decomposition, reactions at electrodes, clogging of microchips, surface interactions, injection and power supply as well as detector-related problems on measurements are discussed. Additionally also strategies for proper analysis and technical solutions are identified.

Consequently, a novel type of high-voltage power supply for quantitative analysis by MCE was developed. This versatile 6 kV instrument has four independent outlets and can be easily adjusted to many desired specifications without changing the whole design. It allows an electrical current of 1 mA and switches from 0 to 6 kV in less than 50 ms. With this device, the benefits of high potentials for MCE separations have been demonstrated.

The use of microchip capillary electrophoresis for routine analysis of real samples has been demonstrated by the development of two analytical methods for different types of samples. The first method quantifies thiols as the active ingredient in depilatory cream and cold-wave lotion. Second, the amount of taurine as component of energy and sports drinks was determined. In both cases, fluorogenic reagents were used to stabilize the reactive molecules and to obtain lower limits of detection. A wavelength-resolved detection system was used to differentiate between analyte and impurities in the taurine example. Comparison with independent HPLC measurements showed good agreement with the data obtained by the microchip-based method.

Furthermore, the affinity of different cyclodextrin vesicles to an adamantane carboxylate guest was examined by capillary electrophoretic methods. The molecular recognition of adamantane carboxylate turned out to be specific to β -cyclodextrins as a binding constant of $K_a = 7.1 \times 10^3 \text{ M}^{-1}$ was determined. γ -Cyclodextrin vesicles showed lower binding ($K_a = 3.2 \times 10^3 \text{ M}^{-1}$), and for α -cyclodextrins or even non-cyclodextrin vesicles no specific affinity towards the guest molecules (both: $K_a \sim 100 \text{ M}^{-1}$) was detected.

Samenvatting

Dit proefschrift beschrijft de ontwikkeling van nieuwe instrumenten en analytische methoden voor kwantitatieve capillaire elektroforese op microchip (MCE). Een groot voordeel van de op microchip gebaseerde methode is het sterk gereduceerde verbruik van chemicaliën en monsters. Hoge-snelheidsscheidingen zijn uitgevoerd bij een hoge aangelegde potentiaal. Daarvoor is een flexibele hoogspanningsbron nodig zoals is ontwikkelt in deze dissertatie.

Een inleidend overzicht geeft de algemene eisen van capillaire elektroforese (CE) op microchip weer. Het verschil tussen op chip gebaseerde CE en conventionele CE wordt verklaard aan de hand van buffer-decompositie, elektrode reacties, geblokkeerde microchips, wisselwerking met de oppervlakte, de spanningsbron, de injectie en problemen met de detectie. Niet alleen zijn de struikelpunten verklaard, maar ook de mogelijkheden voor passende analyse en technische oplossingen worden aan het licht gebracht.

Voor kwantitatieve MCE is vervolgens een nieuw type hoogspanningsbron ontwikkeld met vier onafhankelijke uitgangen voor maximaal 6 kV. Door het veelzijdige design kan er makkelijk worden gevarieerd tussen diverse specificaties zonder een compleet nieuw instrument te hoeven ontwerpen. Het instrument laat een stroomsterkte van 1 mA toe en schakelt van 0 naar

6 kV binnen 50 ms. Met dit nieuwe apparaat zijn de voordelen van een hoog voltage voor op chip gebaseerde scheidingen aangetoond.

De toepassing van capillaire elektroforese op microchip voor reële monsters is gedemonstreerd middels de ontwikkeling van scheidingsmethoden voor twee verschillende monsters. In de eerste methode zijn thionen als actieve bestanddelen van ontharingscrème en permanentvloeistof gekwantificeerd. In het tweede voorbeeld is de hoeveelheid taurine in sport- en energiedranken gemeten. Beide analyses zijn met een fluorescerend reagens doorgevoerd. Voor de taurinebepaling is een detectiesysteem met golflengteresolutie gebruikt om onderscheid te maken tussen analytmolekullen en verontreinigingen. De vergelijking van de MCE resultaten met onafhankelijke HPLC-metingen leverde voor beide methoden een goede overeenstemming.

Tenslotte is de affiniteit van verschillende cyclodextrinevesicles voor een adamantaancarboxylaat-gast onderzocht met behulp van capillaire elektroforese. De moleculaire herkenning van adamantaancarboxylaat blijkt specifiek te zijn voor β -cyclodextrinevesicles op basis van de gevonden bindingsconstante van $K_a = 7.1 \times 10^3 \text{ M}^{-1}$. γ -cyclodextrine vertoont een lagere affiniteit ($K_a = 3.2 \times 10^3 \text{ M}^{-1}$) en voor α -cyclodextrine of vesicles van niet-cyclodextrines is geen specifieke binding vastgesteld (voor beide: $K_a \sim 100 \text{ M}^{-1}$).

Acknowledgement

The work on this thesis started in February 2003 in the Chemical Analysis Group at the University of Twente in Enschede. After moving to the University of Münster for the last year of research, my time as a PhD student comes to an end and the thesis is finally finished. Therefore I would like to thank a number of people who helped me to finish this thesis.

I thank Uwe for guiding me through an interesting and challenging research topic during the last years. He was involved in many scientific discussions, managed to provide a good working atmosphere and enabled many valuable trips to scientific conferences and courses.

My special thanks go to my colleagues in the chemical analysis group, who helped me not only on the analytical side of life. In Enschede these are: Annemarie, Bettina and Christel for being my mates in the “Kükenbüro“, Heiko, Hartmut for being as he is, Martijn for being CE too, Martin for offering his “Rechtschreib- und Grammatikprüfung“, Nancy for ordering everything except chocolate, Rasmus, Sebastian for sharing the struggle with microchips, Susanne, Suze and Tanja. Unfortunately I also have to thank André for this word and being receptive for a “Kleines“.

Acknowledgement

In Münster I thank Andy for sharing his music with 219, Anna and Annika for bringing “food” to the chemistry, Bettina, Suze and Martin for being there again, Carsten, Jens for helping to plant palm trees in our lab and Björn for trying to poison them, Joris, Marianne, Michael H., Michael K. for anticipating totally different problems on the same topic, Nils, Wiebke for being round the corner, Sascha, Stefan, Susanne, Torsten and Wolfgang.

I also want to thank the students who assisted me during my research: Sander, Zipeng, Manuel, Stefan, Ilona, Hella and Lydia.

Last but not least I thank Angela and my family for their mainly non-scientific support during this period of my life.

Curriculum Vitae

Personal Details

Name: Tobias Revermann
Nationality: German
Date of Birth: April 27th, 1977
Born in: Osnabrück, Germany

Education

1983 – 1987 Friedrich Adolf-Krummacher-Schule, Tecklenburg, Germany

1987 – 1996 Graf-Adolf-Gymnasium, Tecklenburg, Germany
Graduation in June 1996

1996 – 1997 Civilian service

1997 – 2003 Studies of chemistry and food chemistry at the University of Münster, Germany

12 / 1999 Intermediate exam chemistry

01 / 2000 Intermediate exam food chemistry

2001 / 2002 Visiting student at the University of Colorado, Boulder, CO, USA

- 01 / 2003** Graduation in chemistry (Diplom), Thesis:
“Sorbensspezifische Thermodesorption von
Spurenkonzentrationen flüchtiger Kohlen-
wasserstoffe und deren Detektion mit Gassensoren”
(practical work at: Institut für Chemo- und
Biosensorik e. V., Münster, Germany)
- 02 / 2003** Begin of Dissertation in Analytical Chemistry at the
University of Twente (Enschede, The Netherlands)

List of publications

Original papers

T. Revermann, S. Götz, U. Karst: "Microchip Capillary Electrophoresis for Quantitative Analysis", submitted for publication.

M. Kießhauer, T. Revermann, J. Künnemeyer, U. Karst: „Extendable Four Channel High-Voltage Power Supply for Fast Microchip Capillary Electrophoretic Separations”, submitted for publication.

T. Revermann, S. Götz, U. Karst: "Quantitative Analysis of Thiols in Consumer Products on a Microfluidic Capillary Electrophoresis Chip with Fluorescent Detection", *Electrophoresis*, **2007**, accepted for publication.

S. Götz, T. Revermann, U. Karst: "Quantitative On-Chip Determination of Taurine in Energy and Sports Drinks", *Lab Chip*, **2007**, 7, 93-97.

P. Falvey, C. W. Lim, R. Darcy, T. Revermann, U. Karst, M. Giesbers, A. T. M. Marcelis, A. Lazar, A. W. Coleman, D. N. Reinhoudt, B. J. Ravoo: "Bilayer Vesicles of Amphiphilic Cyclodextrins: Host Membranes That Recognize Guest Molecules", *Chem. Eur. J.* **2005**, 11, 1171-1180.

D. Helmig, T. Revermann, B. Hall: "Characterization of a Pressurized C5 - C16 Hydrocarbon Gas Calibration Standard for Air Analysis", *Anal. Chem.* **2004**, 76, 6528-6534.

D. Helmig, F. Bocquet, J. Pollmann, T. Revermann: "Analytical techniques for sesquiterpene emission rate studies in vegetation enclosure experiments", *Atmos. Environ.* **2004**, 28, 557-572.

D. Helmig, T. Revermann, J. Pollmann, O. Kaltschmidt, A. Jiménez Hernández, F. Bocquet, D. David: "Calibration system and analytical considerations for quantitative sesquiterpene measurements in air", *J. Chromatogr. A* **2003**, 1002, 193-211.

Oral presentations

T. Revermann, S. Götz, U. Karst: "Quantitative Microchip Capillary Electrophoresis of Labeled Thiols", Pittcon 2006, Orlando, FL, USA, February 12 – 17, 2006.

T. Revermann, S. Götz, U. Karst: "Quantitative Mikrochip-Kapillarelektrophorese von Thiolen", Seminar for Ph. D. students of the "AK Separation Science (GDCh)", Hohenroda, Germany, January 8 – 10, 2006.

T. Revermann, S. Götz, U. Karst: "Capillary and Microchip Electrophoresis of Thiols after Fluorescence Labeling with Benzoxadiazoles", Pittcon 2005, Orlando, FL, USA, February 27 – March 4, 2005.